ORNL/TM-2023/2925

R-MATRIX ANALYSIS AND STATISTICAL PROPERTIES OF DYSPROSIUM ISOTOPES IN THE NEUTRON ENERGY RANGE UP TO A FEW KEV

Marco T. Pigni

June 2023

OAK RIDGE National Laboratory

ORNL IS MANAGED BY UT-BATTELLE LLC FOR THE US DEPARTMENT OF ENERGY

DOCUMENT AVAILABILITY

Reports produced after January 1, 1996, are generally available free via US Department of Energy (DOE) SciTech Connect.

Website: www.osti.gov/

Reports produced before January 1, 1996, may be purchased by members of the public from the following source:

National Technical Information Service
5285 Port Royal Road
Springfield, VA 22161
Telephone: 703-605-6000 (1-800-553-6847)
TDD: 703-487-4639
Fax: 703-605-6900
E-mail: info@ntis.gov
Website: http://classic.ntis.gov/

Reports are available to DOE employees, DOE contractors, Energy Technology Data Exchange representatives, and International Nuclear Information System representatives from the following source:

Office of Scientific and Technical Information
PO Box 62
Oak Ridge, TN 37831
Telephone: 865-576-8401
Fax: 865-576-5728
E-mail: report@osti.gov
Website: http://www.osti.gov/contact.html

ORNL/TM-2023/2925

Nuclear Criticality Safety Program

R-MATRIX ANALYSIS AND STATISTICAL PROPERTIES OF DYSPROSIUM ISOTOPES IN THE NEUTRON ENERGY RANGE UP TO A FEW KEV

Marco T. Pigni

May 2023

Prepared by
OAK RIDGE NATIONAL LABORATORY
Oak Ridge, TN 37831-6283
managed by
UT-Battelle LLC
for the
US DEPARTMENT OF ENERGY
under contract DE-AC05-00OR22725

CONTENTS

LIST OF FIGURES

LIST OF TABLES

ABBREVIATIONS

BW	Breit–Wigner
ENDF	Evaluated Nuclear Data File
LINAC	Linear Accelerator
NIST	National Institute of Standards and Technology
NCSP	Nuclear Criticality Safety Program
ORNL	Oak Ridge National Laboratory
RM	Reich–Moore
RPC	resonance parameter covariance
RPI	Rensselaer Polytechnic Institute
RRR	Resolved Resonance Region
ToF	Time-of-Flight

ACKNOWLEDGMENTS

This work was supported by the Nuclear Criticality Safety Program, which is funded and managed by the National Nuclear Security Administration for the US Department of Energy. The author also thanks Devin Barry and Robert Block for helpful discussions on the RPI measurements and related experimental corrections.

ABSTRACT

In support of the Nuclear Criticality Safety Program, a set of evaluated resonance parameters was generated for seven dysprosium isotopes in the neutron energy range from thermal up to a few keV. The evaluation methodology used the Reich-Moore approximation to fit, with the *R*-matrix code SAMMY, the high-resolution capture and transmission measurements on natural and enriched samples recently performed at the Rensselaer Polytechnic Institute Gaerttner LINear ACcelerator facility. Additional transmission data measured on enriched samples by Liou at the Columbia University Nevis synchrocyclotron in the mid seventies were used to gauge the neutron widths above 15 eV. Thermal constants such as absorption and (in)coherent scattering cross sections and corresponding scattering lengths were calibrated to the National Institute of Standards and Technology's compilation except for ^{161,164}Dy isotopes.

1. INTRODUCTION

Named from the Greek *dysprositos* meaning "hard to get," dysprosium is a rare earth element that can have significant effect in nuclear reactor applications due to its property of absorbing neutrons continuously and effectively for a long time. In fact, because of its large capture cross section, dysprosium is usually exploited in the design of nuclear fuel or reactor control rods, for which dysprosium's slow-burnout property is necessary. Being a rare earth element, dysprosium's capture cross section is also important in the study of nucleosynthesis in astrophysics analyses. Among other common uses, dysprosium (in compound forms or dysprosium alloys) is in great demand because of its favorable thermophysical properties, as dysprosium resists demagnetization at high temperatures.

In view of the interest in dysprosium metal for several distinct types of nuclear applications, it is important to have a thorough understanding of its interaction with neutrons. To describe the reaction cross sections in the thermal and low-energy range, resonance parameters are usually stored in evaluated nuclear data file (ENDF) libraries. In the recently released ENDF/B-VIII.0 nuclear data library [1], the set of dysprosium evaluations in the resolved resonance region (RRR) was performed in 2001 (after the release of the ENDF/B-VI.8 library) and successively adopted by two releases of ENDF library—namely, ENDF/B-VII.0 [2] and -VII.1 [3]. Evaluated by the unfavorable multilevel Breit–Wigner (BW) approximation, the set of resonance parameters was adopted from the work of Mughabghab [4], except minor corrections to the bound levels were performed so as to reproduce more accurately the values of the thermal capture cross sections and the bound coherent scattering lengths. Among other experimental data sets, Mughabghab's set of resonance parameters were mainly evaluated on the basis of high-resolution neutron time of flight spectroscopy measurements performed at the Columbia University Nevis synchrocyclotron in the mid seventies [5].

Following the evaluation work performed by Lee in the mid 2000s [6] and the series of recent transmission and neutron capture yield measurements on enriched and natural Dy samples performed at the Gaerttner LINear ACcelarator (LINAC) facility at Rensselaer Polytechnic Institute [7, 8], this work presents the newly evaluated set of neutron resonance parameters for total and capture cross sections on $^{156,158,160\text{–}164}$Dy isotopes in the energy range of thermal energy up to a few keVs. The analysis of the experimental data sets uses the SAMMY [9] code, which performs a multi-level, multi-channel *R*-matrix fit to neutron data in the Reich–Moore (RM) formalism. Experimental conditions such as resolution function, finite sample size, nonuniform thickness, detector efficiencies and nuclide abundances of sample, multiple scattering, self-shielding, normalization, background, and Doppler broadening are taken into account. From both the capture and transmission data, we determined pertinent resonance parameters—and from these, the values of their systematics, such as strength functions, level spacings, and cumulative plots. In the thermal energy range, we utilized the *Atlas of Neutron Resonances* [10] as well as the coherent scattering lengths published by the National Institute of Standards and Technology (NIST) as a source of information on scattering and capture cross sections, as well as the resonance integral.

The report is organized as follows. The general conditions and evaluation methodology are outlined in Section 2, including two extensive subsections about the quantification of the external functions and thermal characteristics of the Dy isotopes; the experimental database is described in Section 3; the calculations and results of the *R*-matrix analysis are presented and discussed in Section 4, followed by a section on the uncertainty quantification. Statistical properties of the resonance parameters and their average values are examined in Section 5 and, for reproducibility purposes, a brief discussion on the repository generated to store and reproduce the results of this work is given in Section 4.1, followed by our conclusions and recommendations in Section 7.

2. GENERAL CONDITIONS AND EVALUATION METHODOLOGY

2.1 DYSPROSIUM ISOTOPES

Naturally occurring dysprosium ^{nat}Dy consists of seven stable isotopes, $^{156,158,160–164}$Dy, plus an extremely long half-life isotope, ^{154}Dy ($t_{1/2} = 3 \times 10^{+6}$ y). The even-A stable isotopes have spin-parity $I^{\pi} = 0^{+}$ that couples to s-wave neutrons to make compound nuclear states all characterized by the same spin parity $J^{\pi} = 1/2^{+}$, whereas the two odd-A stable isotopes, ^{161,163}Dy having $I^{\pi} = 5/2^{+}$ and $5/2^{-}$, respectively, couple to make two compound nuclear states $J^{\pi} = 2^{+}, 3^{+}$ and $J^{\pi} = 2^{-}, 3^{-}$. Table 1 shows four major Dy isotopes with a relatively homogeneous isotopic distribution. For each isotope, the upper energy limit $E_{\max}$ is based on the systematics of Liou's data sets and corresponds to the energy regions where a large fraction of s-levels began to be experimentally missing. As can be seen, the resolved resonance range for odd-A isotopes extends over a smaller $E_{\max}$ than for even-A isotopes since the latter ones are naturally characterized by a larger level spacings. As reported in Table 1, the threshold energy for the inelastic channel of each isotope should be considered when determining the upper energy limit of the unresolved resonance region (URR). For each isotope, the RRR energy limit is well below that threshold energy; therefore, the total cross section is defined by only two energetically possible channels, elastic scattering and neutron capture. Although not planned in the list of nuclei relevant to NCSP, two minor isotopes, ^{156,158}Dy, were included in the R-matrix analysis for completeness. This set of isotopes occurs in the mass region of the split 4s giant resonance in

Table 1. Dysprosium abundances (in %), upper energy limits for the RRR, and inelastic threshold energies (in keV).

No.	Isotope (I^{π})	Abundance (%)	$E_{\max}$ (keV)	E_{inl} (keV)
1 (*)	^{156}Dy (0^{+})	0.056	0.1	137.8
2 (*)	^{158}Dy (0^{+})	0.095	0.1	98.9
3	^{160}Dy (0^{+})	2.329	2.0	80.6
4	^{161}Dy ($5/2^{+}$)	18.889	1.0	25.6
5	^{162}Dy (0^{+})	25.475	5.0	80.6
6	^{163}Dy ($5/2^{-}$)	24.896	1.0	73.4
7	^{164}Dy (0^{+})	28.260	7.0	73.4

(*) Not planned by NCSP.

the S_0 strength function where the S_1 strength functions are expected to be smaller, so the observed level populations are nearly complete s-level populations, with little or no p-level contamination. In fact, with the current experimental data sets, only a few p-wave resonances were observed, and the evaluated set of resonance parameters is practically a pure single population of s levels.

2.2 QUANTIFICATION OF THE EXTERNAL FUNCTIONS

The R-matrix theory shows that the reaction cross sections analyzed over a limited energy range do not depend only on the "internal" levels but also on contributions from "external" levels below and above that energy range [11]. Therefore, before performing the R-matrix fit of the resonance parameters, it is important to quantify the contribution of the resonance analysis below the energy $E_{\min}$ (usually chosen as the zero energy) and above $E_{\max}$, which is generally the upper energy limit where measured data can be still analyzed without losing statistical information on resonance levels. These two energies represent the energy limits of the analyzed neutron range, and the external contribution can be achieved quite conveniently by a resonance statistical representation of the external levels approximated by the tails of two very broad resonances with equal strength [11]. Namely, for s-wave and $\overline{\Gamma}_\gamma \ll I$, this yields external levels with neutron widths

$$\Gamma^J_{\mathrm{n}\pm} = \frac{3}{2} I S^J_0 \sqrt{\frac{|E_\pm|}{1\ \mathrm{eV}}}\,, \tag{1}$$

located symmetrically with respect to the mid-energy $\overline{E} = (E_{\max} + E_{\min})/2$ of the length of the interval $I = (E_{\max} - E_{\min})$ containing the local levels and calculated at energies $E_\pm = \overline{E} \pm \sqrt{3}I/2$. The value of the s-wave strength function S^J_0 for different spin populations (two for odd-A isotopes such as ^{161,163}Dy) can be obtained by the statistical analysis of the known widths of the resonance parameters. In Table 2, the values of the neutron widths and related energy levels calculated with Eq. (1) are reported along with the neutron s-wave strength functions obtained from ENDF/B-VIII.0 resonance parameters.

Table 2. External function parameters calculated with Eq. (1) including the strength functions S^J_0 (in 10^{-4} units), the corresponding pole strength s^J_0 (in 10^{-2} units)*, the length interval I (in keV) and related resonance widths ($\Gamma_{\mathrm{n}\pm}$ in meV) for each channel spin J^π.

Isotope (I^π)	I	E_-	$\Gamma^J_{\mathrm{n}-}$	E_+	$\Gamma^J_{\mathrm{n}+}$	S^J_0	s^J_0	J^π
^{160}Dy (0^+)	2.0	−732	15909	2732	30734	1.96	6.01	$1/2^+$
^{161}Dy ($5/2^+$)	1.0	−366	2739	1366	5291	0.95	2.92	2^+
			2304		4452	0.80	2.46	3^+
^{162}Dy (0^+)	5.0	−1793	66924	6693	129286	2.15	6.58	$1/2^+$
^{163}Dy ($5/2^-$)	1.0	−366	3415	1366	6597	1.19	3.65	2^-
			2447		4727	0.85	2.61	3^-
^{164}Dy (0^+)	7.0	−2562	70688	9562	136559	1.33	4.07	$1/2^+$

(*) The strength function and the pole strength are related by the channel radius a_c and wave number $k_c \equiv k_c(E)$ for the channel c as $S^J_\ell = 2a_c k_c s^J_\ell \sqrt{1\mathrm{eV}/E}$.

The R-matrix external level representation obtained by two broad resonances with equal strength is quite convenient; however, it is an approximation to the R-matrix function

$$R_{cc}(E) - R^\infty_c = 2s_c\left\{\tanh^{-1}\left[\frac{E-\overline{E}}{I/2}\right] + i\frac{\overline{\Gamma}_\gamma}{I}\left[1-\left(\frac{E-\overline{E}}{I/2}\right)^2\right]^{-1}\right\} \simeq \frac{\gamma^2_{\mathrm{n}-}}{E_- - E - i\overline{\Gamma}_\gamma/2} + \frac{\gamma^2_{\mathrm{n}+}}{E_+ - E - i\overline{\Gamma}_\gamma/2}\,, \tag{2}$$

where $\overline{\Gamma}_\gamma$ is the average capture width, R^∞_c is the distant-level parameter, and the reduced amplitude is related to resonance neutron widths as $\Gamma^c_{\mathrm{n}\pm} = 2P_\ell(E_\pm)\gamma^2_{c\mathrm{n}}$ as defined in Eq. (1). Although the differences between the two representations are usually small over most of the energy range, the differences are not negligible towards the edges. To correct for the edge effects of the approximation of Eq. (2), it is necessary to include additional bound and external levels to those of Table 2. Starting from the resonance parameters of Table 2 plus one additional bound and external level for each channel group, a fit of the elastic cross sections calculated from the R-function $R_{cc'}(E) \equiv R_{cc'}$ was performed over the energy interval I for each isotope. The fit of the calculated elastic cross sections was performed by varying the neutron widths and keeping unchanged the average capture widths. The use of the elastic cross sections was necessary because the SAMMY code cannot account for the complex part of the R-function $R_{cc'}$. In doing so, one assumes that the correlation between the elastic and capture reaction channel is negligible.

This procedure yields the set of resonance parameters of Table 3 and the results of the fit, specifically for the ^{160}Dy isotope, showing the inclusion of the edge effects in the external function; these additional bound and external levels are plotted in Fig. 1. The edge effects of the elastic cross sections calculated by the SAMMY code using the R-function $R_{cc'}$ (in purple) are well reproduced by the cross sections (in light blue), reconstructed from the set of resonance parameters reported in Table 3. The results from the use of the broad levels defined in Eq. (1) are shown in green. One should note that the parameters reported in Table 3

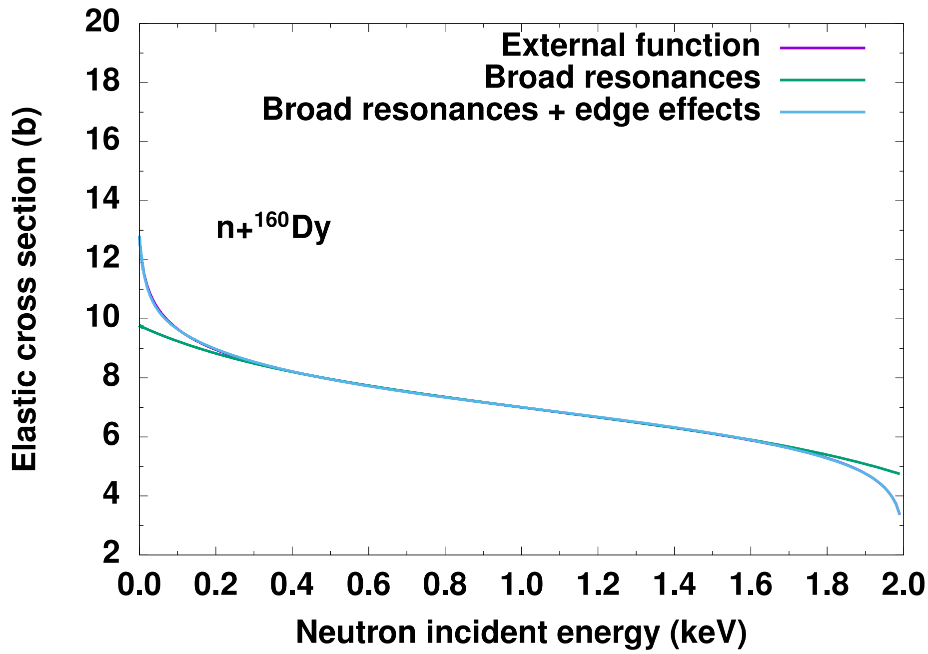

Figure 1. n+^{160}Dy elastic cross sections showing the inclusion of the edge effects. The elastic cross sections calculated by the SAMMY code using the R-function $R_{cc'}$ are shown in purple. In light blue and green are the results of the elastic cross sections reconstructed from the resonance parameters with or without edge effects, respectively.

represent the initial set of external parameters. This is usually modified following the fit of the complete set of measured data and, most importantly, the calibration of the thermal values for scattering, capture, and fission (only for fissile nuclei) reaction channels.

2.3 DYSPROSIUM THERMAL CHARACTERISTICS

The calibration of the negative (or bound) energy levels and related resonance widths was achieved by fitting Block's transmission and capture data [7] measured on ^{nat}Dy samples together with the reference thermal characteristics of each isotope reported by Sears [12], which are also available on the NIST website. As shown in Fig. 3, Block's measured capture and transmission data nicely extend to the thermal energy below 1 eV and, together with Sears' thermal constants, can be excellent constraints in defining the resonance parameters—particularly for negative energies. In doing so, an important aspect of the fitting procedure is the inclusion of relevant experimental corrections related to the detector deficiencies for the capture yield measurement, as these corrections are particularly sensitive to the low-energy tail of the measured data. These are described in detail in Ref. [7] and used in SAMMY inputs as the scaling factor for each isotope.

Table 3. Resonance parameter for initial external function quantification with edge effects. Resonance parameters (in meV) and resonance energies (in eV) obtained by the fit of the elastic cross sections calculated from the R-function $R_{cc'}$ of Eq. (2).

Isotope (I^{π})	E_{min}	E_{max}	E	Γ_{n}^{J}	$\overline{\Gamma}_{\gamma}$	J^{π}
^{160}Dy (0^+)	0.0	2.0	−565.21	10415.69	110	$1/2^+$
			−19.38	46.71		
			2023.03	662.08		
			2587.66	22293.35		
^{161}Dy ($5/2^+$)	0.0	1.0	−358.09	2455.13	120	2^+
			−12.71	23.96		
			1256.15	393.62		
			1347.29	4617.17		
			−361.69	1980.77	120	3^+
			−106.89	43.90		
			1009.96	134.35		
			1345.69	3736.60		
^{162}Dy (0^+)	0.0	5.0	−1294.41	38944.84	120	$1/2^+$
			−62.63	45.16		
			5032.44	1784.12		
			6253.58	86419.92		
^{163}Dy ($5/2^-$)	0.0	1.0	−410.60	2393.04	120	2^-
			1010.92	292.77		
			1349.55	6956.22		
			−382.47	3078.90	120	3^-
			−13.61	29.34		
			1276.95	73.73		
			1359.49	3549.83		
^{164}Dy (0^+)	0.0	7.0	−2036.79	46723.60	100	$1/2^+$
			−99.98	306.77		
			7102.11	1132.59		
			9015.64	98607.11		

This work started from the initial set of the external levels of Table 3 to find the current evaluated resonance parameters for the external energy levels and related channel widths of each isotope, as reported in Table 4. Highlighted in blue are those (negative) levels added to improve the fit of the measured data including thermal constants. Although thermal scattering cross sections and scattering lengths are intimately related, the latter should be always checked to ensure proper calibration with available measured data. In fact, even when the thermal cross sections are satisfactory, the scattering lengths may need additional calibration. Although the SAMMY code does not currently have the capability to fit the scattering length as measured data, this work attempted to calibrate both scattering lengths and scattering cross sections. The evaluated bound (in)coherent scattering lengths and thermal capture cross sections are reported in Table 5 together with the values of complex bound scattering lengths and related radii. In this evaluation work, the scattering or potential radius R′ and the effective radius a_c that is usually used to calculate the penetration factors were kept the same for all channels of each isotope.

Table 4. Resonance parameters for final external function quantification. Highlighted in blue are the energy levels added to improve the fit of the measured data including thermal constants. Units are the same as those in Table 2.

Isotope (I^π)	$E_{\min}$	$E_{\max}$	E	Γ_n^J	$\overline{\Gamma}_\gamma$	J^π
^{160}Dy (0^+)	0.0	2.0	−601.81	9545.25	103	$1/2^+$
			−51.98	326.19	99	
			−14.30	9.05	86	
			2023.00	662.62	110	
			2586.10	22795.48	110	
^{161}Dy ($5/2^+$)	0.0	1.0	−360.67	2454.73	120	2^+
			−19.83	29.88	120	
			1256.13	393.66	120	
			1347.11	4621.42	120	
			−360.67	2453.73	120	3^+
			−110.44	44.55	120	
			−2.50	15.37	150	
			1009.92	134.37	120	
			1345.10	3747.88	120	
^{162}Dy (0^+)	0.0	5.0	−1255.35	13241.10	117	$1/2^+$
			−47.40	38.58	111	
			5032.50	1779.22	120	
			6253.58	78659.40	120	
^{163}Dy ($5/2^-$)	0.0	1.0	−552.74	4151.67	120	2^-
			1007.24	294.93	120	
			1296.58	8631.93	120	
			−584.20	1513.45	120	3^-
			−4.65	3.20	120	
			1275.23	74.83	120	
			1275.50	4883.50	120	
^{164}Dy (0^+)	0.0	7.0	−2037.05	46629.74	83	$1/2^+$
			−102.50	310.25	83	
			−1.88	50.06	63	
			7102.11	1132.61	100	
			9015.64	98653.65	100	

One can find reasonable agreement with the values reported by the NIST compilation except for the cases of the ^{161,164}Dy isotopes. For the most abundant isotope ^{164}Dy, there is a discrepancy of 200 b (about -7%) noticeable for the absorption cross section and 24 b (about $+8\%$) for the scattering cross section leading to a reduction of the thermal value for the total cross section of about 170 b (about -5%). The evaluated thermal capture value was found by fitting the recently measured activation data [13]. For the scattering channel, only a few measured data are available, and the NIST value differs by about 24 b with the ENDF/VIII.0 library. The value of about 331 b evaluated in this work was calibrated and constrained by the simultaneous fit of transmission and capture data for ^{nat}Dy together with thermal capture and scattering constants for six other isotopes. The choice of a larger ^{164}Dy thermal scattering value than that reported by the NIST compilation was also motivated by recent and accurate capture activation measurements. In fact, the ^{164}Dy scattering thermal cross section obtained by the difference between the total cross section, $\sigma_{\text{tot}} = 3000^{-70}_{+45}$ b, measured at thermal by Vertebny [14, 15], and the thermal capture cross section, $\sigma_\gamma = 2650 \pm 25$ b, measured by Farina [13], yields $\sigma_s = 350^{-65}_{+37}$ b. From this, and assuming Farina's recent measured data set is reliable, the NIST compilation value for the ^{164}Dy scattering cross sections is clearly found outside the considerably large derived uncertainty range. On a different note related to the 4$^{\text{th}}$ most abundant isotope, the scattering cross section of the ^{161}Dy isotope is still 2σ within the NIST compilation and was adopted from the ENDF/B-VIII.0 library based on the goodness of the fit of the natural data. This choice is also consistent with the evaluation work by Lee [6].

The following paragraphs report the details of the derivation for the equations used to calculate the thermal constant values reported in Table 5. For the scattering lengths, a convenient way to show their

Table 5. (In)coherent bound scattering(*) and thermal absorption cross sections (in barn) with corresponding bound (in)coherent scattering lengths(**) (in fm) compared to the values reported by NIST(***). The scattering radius a_c (in fm) for each isotope is also reported.

	a_c		σ_γ	σ_s	σ_{coh}	σ_{incoh}	b_{coh}	b_{incoh}	b_+	b_-
^{156}Dy	7.50	Present	33	4.1	4.1	0.0	5.7	0.0	n/a	n/a
		NIST	33	4.7	4.7	0.0	6.1	0.0	n/a	n/a
^{158}Dy	7.40	Present	43.1	6.5	6.5	0.0	7.2	0.0	n/a	n/a
		NIST	43.0	5.0	5.0	0.0	6.0	0.0	n/a	n/a
^{160}Dy	7.46	Present	55	5.6	5.6	0.0	6.7	0.0	n/a	n/a
		NIST	56	5.6	5.6	0.0	6.7	0.0	n/a	n/a
^{161}Dy	7.47	Present	605	17.5	14.5	3.0	$10.7-\imath\,0.17$	$4.9-\imath\,0.12$	$8.71-\imath\,0.16$	2.08
		NIST	600	16.0	13.3	3.0	10.3	4.9	n/a	n/a
^{162}Dy	5.90	Present	195	0.28	0.28	0.0	-1.50	0.0	n/a	n/a
		NIST	194	0.25	0.25	0.0	-1.41	0.0	n/a	n/a
^{163}Dy	7.50	Present	125	3.2	3.2	0.27	4.9	1.3	3.5	1.4
		NIST	124	3.3	3.1	0.21	5.0	1.3	n/a	n/a
^{164}Dy	7.51	Present	2650	327	327	0.0	$51.3-\imath\,0.74$	0.0	n/a	n/a
		NIST	2840	307	307	0.0	$49.7-\imath\,0.79$	0.0	n/a	n/a

(*)By definition, the scattering and coherent cross section are identical for nuclei with spin $I = 0$.
(**)The imaginary component of the calculated bound scattering lengths b is reported for values >0.1.
(***)As discussed in subsection 2.2, the bound scattering lengths and related cross sections can be converted to free quantities by the factor $(A+1)/A$ which, for the Dy isotopes, introduces a difference of about 0.6%. In this work, the contribution of the neutron-electron interaction was not included.

relationship to R-matrix parameters is to expand the collision matrix in the low energy limit. The theoretical values of the reported scattering lengths were calculated on the basis of the collision matrix U^J_{cc} for the elastic channel (c=c') computed from the set of the evaluated resonance parameters and scattering radius R$'$ for each Dy isotope. In the reduced R-matrix approximation, the RM collision function for each s-wave incident neutron channel J=$(I \pm 1/2)^\pi$ (i.e., one for I=0, two for $I \neq 0$);

$$U^J_{cc} = e^{-2\imath k_c a_c}[1 - \imath k_c a_c R^J_{cc}]^{-1}[1 + \imath k_c a_c R^J_{cc}]\,, \tag{3}$$

where the quantity a_c is the radius for the incident channel c (usually chosen to be equal to the potential scattering radius R$'$), and k_c=$\alpha_c \sqrt{E}$ is the wave number defined for the incident (neutron) channel, namely, for α_c=$2.1968\times10^{-4}A_c/(A_c+1)$ (in fm^{-1} eV$^{-1/2}$): E is expressed in eV, and α_c is the nucleus–neutron mass ratio for particle pair of the incident channel. The reduced-R complex function for this one-channel case is

$$R^J_{cc} = \sum_\lambda \frac{\gamma^2_{\lambda(J,c=\mathrm{n})}}{E_\lambda - E - \imath\Gamma_{\lambda\gamma}/2}\,, \tag{4}$$

where the summation extends over the nuclear energy (positive and negative) levels E_λ related to the formal energy states of the nuclear compound system with reduced neutron width amplitude $\gamma_{\lambda\mathrm{n}}$ and capture widths $\Gamma_{\lambda\gamma}$. Omitting the index c being the quantities corresponding to the (neutron) elastic scattering, the collision function in the low-energy limit, x=$ka \to 0^+$, can be written as

$$U^J = 1 + 2\imath x\,(R^J - 1) - 2x^2(R^J - 1)^2 + o(x^3)\,. \tag{5}$$

Comparing the detailed and usual form of the elastic scattering wave function for s-wave neutron interaction, one can obtain the relation between the scattering wave amplitude and the RM collision function,

$$\mathrm{F}^J = \imath a\,(1 - U^J)/(2x), \tag{6}$$

which is related to the free scattering length for the channel spin J as

$$\mathrm{a}^J = -\lim_{x\to0^+} \mathrm{F}^J \approx a\,[1 - \Re(R^J) - \imath\Im(R^J)] = a\,(1 - R^J)\,. \tag{7}$$

For nuclei with target spin $I = 0$, the free coherent scattering length is the quantity defined in Eq. (7); however, for nuclei with target spin $I \neq 0$, the free coherent scattering length

$$\mathrm{a}_{\mathrm{coh}} = \begin{cases} \mathrm{a}^J & I = 0 \\ g_+\mathrm{a}^{J_+} + g_-\mathrm{a}^{J_-} & I \neq 0 \end{cases}$$

is the sum of the partial scattering lengths weighted by their spin statistical factors $g_+ = (I+1)/(2I+1)$, $g_- = I/(2I+1)$ related to $J_+ = I + 1/2$ and $J_- = |I - 1/2|$, respectively. The same quantities are also used to compute the incoherent scattering length, defined as

$$\mathrm{a}_{\mathrm{incoh}} = \begin{cases} 0 & I = 0 \\ \sqrt{g_+g_-}(\mathrm{a}^{J_+} - \mathrm{a}^{J_-}) & I \neq 0\,. \end{cases}$$

Since the measured or recommended data are usually reported as bound (in)coherent scattering length $\mathrm{b}_{\mathrm{(in)coh}}$, the relation used in this work to convert the measured quantities to free (in)coherent scattering lengths is $\mathrm{a}_{\mathrm{(in)coh}} = \mathrm{b}_{\mathrm{(in)coh}}\,A/(A+1)$, ,from which one can calculate the free scattering cross section

$$\sigma_{\mathrm{s}} = 4\pi \begin{cases} |\mathrm{a}^J|^2 & I = 0 \\ g_+|\mathrm{a}^{J_+}|^2 + g_-|\mathrm{a}^{J_-}|^2 & I \neq 0\,, \end{cases}$$

where, for $I \neq 0$, the result is given by the unitary condition of the spin statistical factors, $g_+ + g_- = 1$, and the sum of the coherent and incoherent cross sections,

$$\sigma_{\mathrm{coh}} = 4\pi\,|g_+ \mathrm{a}^{J_+} + g_- \mathrm{a}^{J_-}|^2 \quad \text{and} \quad \sigma_{\mathrm{incoh}} = 4\pi\, g_+ g_-\, |\mathrm{a}^{J_+} - \mathrm{a}^{J_-}|^2\,. \tag{8}$$

In the case of the Dy isotopes, the absorption cross section is given by the capture reaction channel only, and, as reported in Table 5, the value calculated from the free scattering length is defined by

$$\sigma_\gamma = \frac{4\pi}{k}\begin{cases} |\Im(\mathrm{a}^J)| & I = 0 \\ g_+|\Im(\mathrm{a}^{J_+})| + g_-|\Im(\mathrm{a}^{J_-})| & I \neq 0\,, \end{cases}$$

where the wave number k is calculated at the thermal neutron energy E_{th}=0.0253 eV.

3. THE EXPERIMENTAL DATABASE

To improve the accuracy of the Dy evaluations in both thermal and resolved resonance neutron energy ranges, a comprehensive experimental database is needed to evaluate the set of resonance parameters. As schematically reported in Table 6, one can distinguish two major experimental campaigns for the Dy isotopes. Chronologically, the first one was performed by Liou [5] at the Columbia University Nevis synchrocyclotron. This included transmission and capture measurements of $^{160-164}$Dy isotopes on enriched Dy_2O_3 samples of different thicknesses focusing on epithermal incident neutron energy range, that is, above 15 eV and up to several keVs. The second experimental campaign was generated within the needs of the NCSP and performed at the Gaerttner LINAC Center at RPI over thermal and epithermal ranges. Among these recent measurements, neutron capture yields of $^{161-164}$Dy isotopes were measured in the energy range from 10 eV up to 1 keV. The capture yield measurements were performed on isotopically-enriched dysprosium metallic samples using the Time-of-Flight (ToF) method with a 16 segment sodium iodide multiplicity detector [8]. Within the same campaign, an additional series of capture and transmission measurements was performed on $^{\mathrm{nat}}$Dy samples in the thermal neutron energy region up to 20 eV [7]. More details on both series of measurements can be found in Refs. [7, 8]. Among the neutron transmission experimental data available for Dy isotopes, Liou's measured data represent a relevant portion because of their extended energy range and sample isotopic enrichment. In fact, Liou's transmission data are currently the only source of information to evaluate the neutron widths of the Dy isotopes in the energy range above 15 eV. Unfortunately, the capture data for this set of measurements are missing, and there is no uncertainty quantification for the transmission data reported in the EXFOR library. Moreover, the large number and magnitude of negative values found in the reported ^{160,163,164}Dy total measured cross sections implies an over-correction of the background contribution. Among possible background corrections, one might have been applied to eliminate the contribution of the oxygen cross sections due to the use of oxide samples Dy_2O_3 in the measurements. In this regard, it is unclear whether the number of atoms/barn reported is related to the specific enriched isotope or to the oxide sample: this affected our ability to correctly calculate the total number of atoms/barn of the samples. Moreover, especially in the low-energy region above 15 eV, the energy spectrum of the Dy isotopes contains several energy levels for which the neutron absorption is maximum. For these levels, Liou's data were reported as saturated resonances because of the choice of the sample thickness, and an accurate fit of the resonance widths was not possible. At least for the resonance levels large enough to be visible with measurements with $^{\mathrm{nat}}$Dy sample, this problem was partially resolved by Shin's transmission data.

Because Liou's transmission data were reported as total cross sections for the whole set of Dy isotopes, the conversion to transmission data was necessary to convolute in the R-matrix analysis the experimental

Table 6. Selected measurements and related sample configurations such as thickness *n* (a/b), path length *L*, and enrichment used in the evaluation of the resonance parameter of Dy isotopes.

Author (year)	Facility	Sample	Type	n (10^{-3} a/b)	Energy range	Path length L (m)
Liou (1975)	NEVIS	^{160}Dy	Trans*	0.881	15 eV–2 keV	202.05
		^{161}Dy		1.644, 7.451	15 eV–1 keV	
		^{162}Dy		1.533, 6.934	15 eV–5 keV	
		^{163}Dy		1.403	15 eV–1 keV	
		^{164}Dy		10.54, 2.337	15 eV–7 keV	
Shin (2017)	RPI	^{161}Dy	Yield	0.6359	12 eV–1 keV	25.57
		^{162}Dy		0.6445	10 eV–1 keV	
		^{163}Dy		0.6503	10 eV–1 keV	
		^{164}Dy		0.6196	10 eV–1 keV	
Block (2017)	RPI	^{nat}Dy	Trans	1.610	0.01–20 eV	14.97
		^{nat}Dy	Yield	0.8050	0.01–20 eV	25.44
		^{nat}Dy	Trans	0.7840	4 eV–2 keV	25.60
		^{nat}Dy	Yield	1.6304	10 eV–1 keV	25.57

(*) Converted to transmission data from the reported total cross sections.

configuration of Liou's measurements. In this regard, the experimental resolution and Doppler broadening parameters were also needed as input parameters for an accurate description of the shape of the experimental data. For Liou's data, only partial information on the set of experimental resolution parameters was found. This consisted of the minimum channel width of Δ_G= 40 ns and the flight path length L = 202.5 m. With this information together with the relation between the energy and the speed of the neutron of mass m,

$$t(E) = \sqrt{\frac{m}{2E}}\,L\,, \tag{9}$$

the values of the crunch data table were directly extracted from Liou's data sets to obtain the energy dependence of the experimental resolution. As shown in Fig. 2 for ^{160}Dy measured data, the number of the energy boundaries $B_{\Delta_G}(E)$ and their related values are clearly distinguishable.

Although the crunch tables were correctly deduced from the data, the impact of the resolution broadening on the transmission data reconstructed including the experimental resolution parameters was not particularly evident. This might suggest that the reported measured data are not exactly the raw measured data but total cross sections reconstructed from the resonance parameters. This would explain the lack of experimental uncertainty analysis in the EXFOR library.

The recent measurements performed on ^{nat}Dy samples at the RPI facility for both transmission and capture yield data supplied additional and relevant information in evaluating the low-energy data in the thermal range and resonance levels up to 20 eV as shown in Fig. 3. However, the natural data measured in the epithermal range up to 2 keV could not match the neutron resonance level information of Liou's isotopically-enriched measurements. In this regard, considerable spectroscopic information obtained from Liou's measurements supported RPI capture yield measurements performed on isotopically-enriched samples.

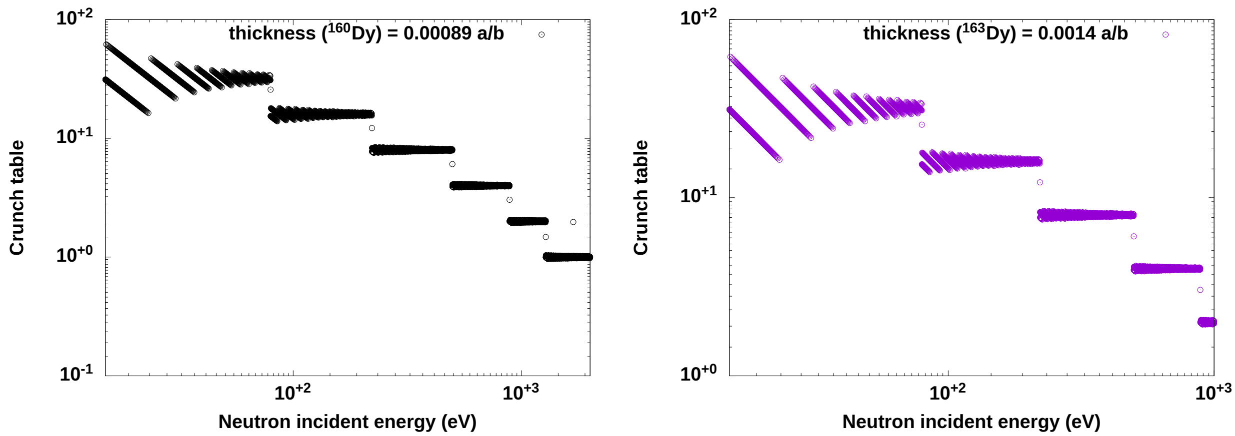

Figure 2. Energy dependent values of the crunch table for a channel width Δ_G=40 ns as a function of the incident neutron energy for the even-*A* isotope ^{160}Dy and odd-*A* isotopes ^{163}Dy.

4. RESULTS OF THE *R*-MATRIX ANALYSIS

The set of RM resonance parameters obtained by the multi-isotopic and multi-channel SAMMY *R*-matrix analysis of Dy experimental data in the energy range from thermal to several keVs contains 664 energy levels, 634 in the analyzed energy range, and 30 external resonances including 17 negative levels. The set of resonance parameters for the natural sample is given in the appendix, and most of the energy levels were considered as induced by *s*-wave neutrons. Only a few *p*-wave resonances were included for two even-*A* isotopes ^{162,164}Dy. In deriving the evaluated resonance parameters, particular care was devoted to the thermal energy region up to 20 eV. Here, the set of resonance parameters was constrained by the thermal values recommended by NIST (with the exception of ^{164}Dy) and by Block's transmission and capture measurements that nicely extended in the low-energy range up to 0.01 eV. In addition to the negative levels defined in Section 2.2, the fitting procedure started from the combination of the set of resonance parameters reported in the ENDF/B-VIII.0 library and Shin's paper [8]. In the latter work, 46 new energy levels (29 for ^{161}Dy and 17 for ^{163}Dy) were reported and adopted in this work, although their existence can be sometimes debatable due to the lower and lower statistics of both measured Shin's capture and Liou's transmission data for increasing incident neutron energy. Moreover, in Shin's work, 12 energy levels (six for ^{161}Dy, two for ^{163}Dy, and four for ^{164}Dy) listed in the ENDF/B-VIII.0 library were not observed. These updates were also adopted by this work with the exception of the energy level at 12.7 eV for the ^{161}Dy isotope. This level was reported and confirmed by Block's transmission measurements [7] and not observed in Shin's capture measurements most likely because of the poor statistics of the measurements in this energy range.

As shown in Fig. 3, the capture yield (left) and transmission (right) measurements on ^{nat}Dy samples were invaluable to evaluate the thermal neutron energy region and the first few resonances up to about 20 eV. The energy-dependent residuals (bottom) are overall well within a reasonable acceptance range except below 0.1 eV. The large deviation is due to the non-physical discontinuity in the experimental uncertainty (top) visible at about 0.1 eV. This effect occurs in both transmission and capture measurements approaching a minimal uncertainty $\lesssim$1% and close to 0.1%, respectively. Although generally unremarkable, other discontinuities are visible in the energy regions at about 4 eV for the capture yield data and about 5 eV for the transmission data. Despite the fact that such discontinuities in the experimental uncertainty at about

0.1 eV and 4–5 eV are related to the crunch tables of the measured data, these generate residual variations up to about 10-sigmas and mainly below 0.1 eV. These large residuals are clearly not possible to address due to the extremely low uncertainty coupled with the constrained behavior ($\propto 1/\sqrt{E}$ and $\propto 1/\sqrt{E}$+const for the capture and total reaction channel, respectively) of the evaluated data in the thermal region. In this regard, the experimental configuration of Block's and Shin's capture measured data depends on the detector efficiencies [7, 8] that are taken into account in the SAMMY R-matrix analysis as a multiplicative factor defined for each isotope, accordingly scaling the calculated neutron capture yield. As expected, these factors are very impactful in describing the low-energy tail of the measured data, and, in this work, they were considered constants. In the epithermal energy region, the energy-dependent residuals of the capture yield

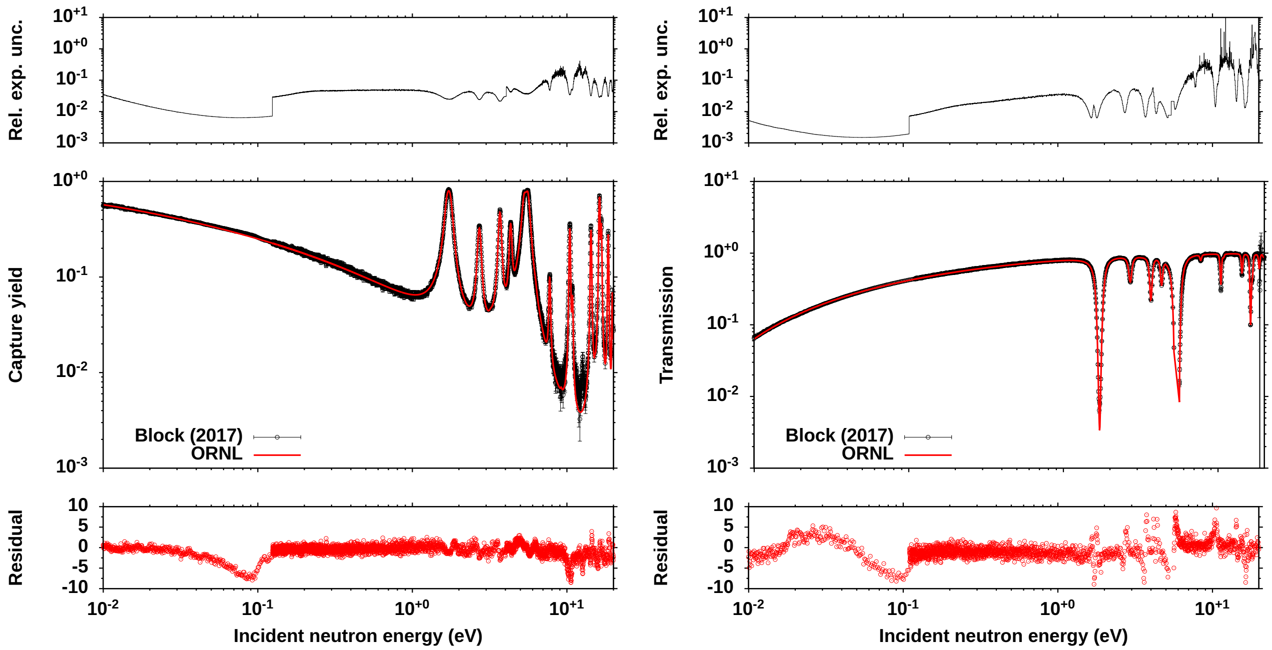

Figure 3. n+^{nat}Dy capture yield (left) and transmission data (right) measured in thermal energy range at the RPI facility (black dots) compared to theoretical data (solid red line). Relative experimental uncertainty (top) and residual (bottom) are shown in black solid lines and red dots, respectively.

and transmission data shown at the bottom of Fig. 4 are on average within 2-sigmas variation range. This is facilitated also by the experimental uncertainty (top) that is larger than previous data measured in the thermal energy range. To avoid clutter in the plotted data, the transmission data measured in the energy region between 300–400 eV where one of the filters' contribution was visible were excluded. Since these measurements performed on ^{nat}Dy samples, only the most relevant resonances were measurable. In this regard, Liou's transmission data [5] as well as Shin's capture yield data [8] measured on enriched samples allow a detailed analysis of the resonance levels for each isotope, as shown in the following figures. As explained in Section 3, Liou's measured data were converted from total cross section to transmission data and, because of no experimental uncertainty was reported, an estimated uncertainty of 1% was assigned to the total cross sections. The transmission data uncertainty was, therefore, based on total cross section estimated uncertainty through the relation $T(E) = e^{-n\sigma(E)}$ together with the corresponding energy-dependent partial derivatives. Clearly, this procedure generates inconsistent uncertainty for both negative total cross sections reported in EXFOR and large saturated resonance levels where the transmission data are nearly zero, and

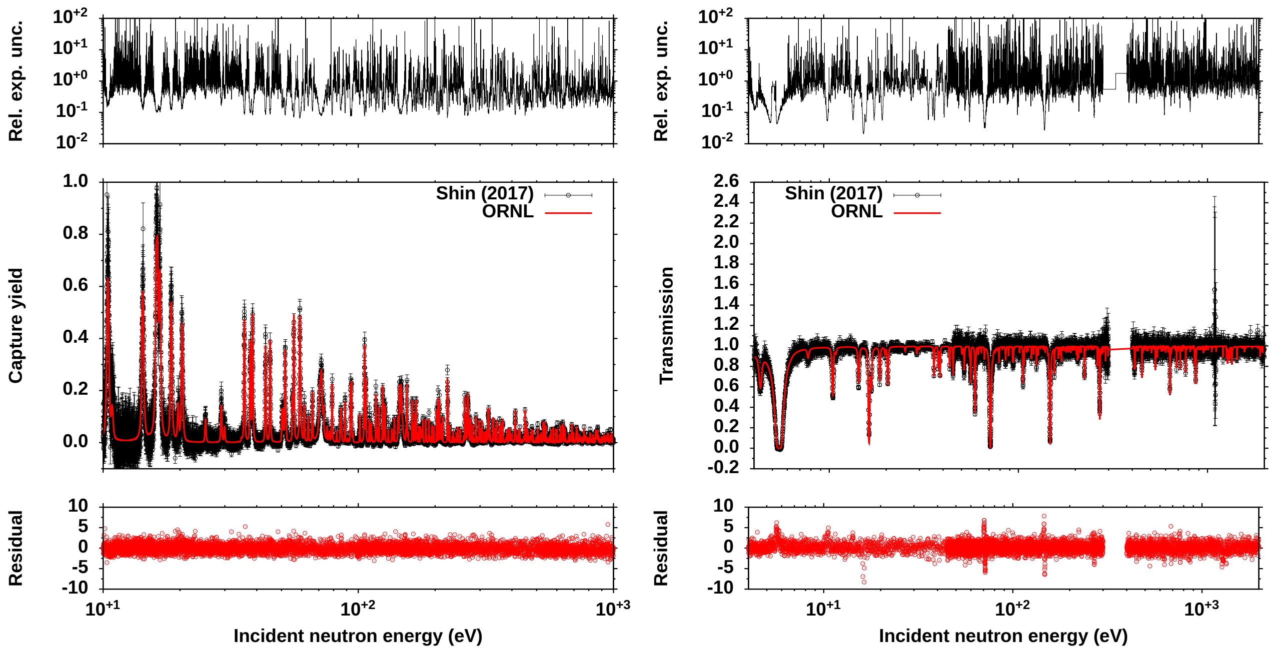

Figure 4. n+^{nat}Dy capture yield (left) and transmission data (right) measured in epithermal energy range at the RPI facility (black dots) compared to theoretical data (solid red line). Relative experimental uncertainty (top) and residual (bottom) are shown in black solid lines and red dots, respectively.

uncertainty could thus be in the range of negative values. Moreover, because the experimental standard deviation is inversely proportional to the square root of the number of events, the assignment of a constant uncertainty does not reflect the fact that in energy regions where large resonance levels are measured, the number of events is considerably higher than in other energy regions (e.g., the valleys). For instance, an expected energy-dependent behavior is clearly shown in the RPI measurements such as Fig. 4, in which a minimum in the capture yield uncertainty corresponds to the peak of the resonance level. In the same figure, the transmission data show a similar behavior—keeping in mind that, by their definition, the minima correspond to the resonance peaks in the total cross sections. For these reasons, Liou's transmission data were not included in the optimization procedure and were used only for their detailed spectroscopic information. In Figs. 5,6,8,10,11, Liou's transmission measured data (in black) with the estimated uncertainties (top) and corresponding residuals (bottom) are plotted together with the calculated data (in red)*.

4.1 UNCERTAINTY QUANTIFICATION

The uncertainty quantification of the evaluated resonance parameters was performed by the Bayesian procedure implemented in the SAMMY code. A sequential Bayesian fit including all (negative and positive) energy levels and related resonance widths for seven isotopes was performed over the set of measured data reported in Table 6 as well as thermal values. The retroactive scheme option was then applied to approximate the covariance matrix obtained in the previous step by assuming the resonance parameters are not very different from one step to another. The generation of a full resonance parameter covariance (RPC) matrix, including the isotope–isotope correlations, would have been the preferable solution. However, due to the

*In these plots, the data associated with negative reported experimental values are eliminated.

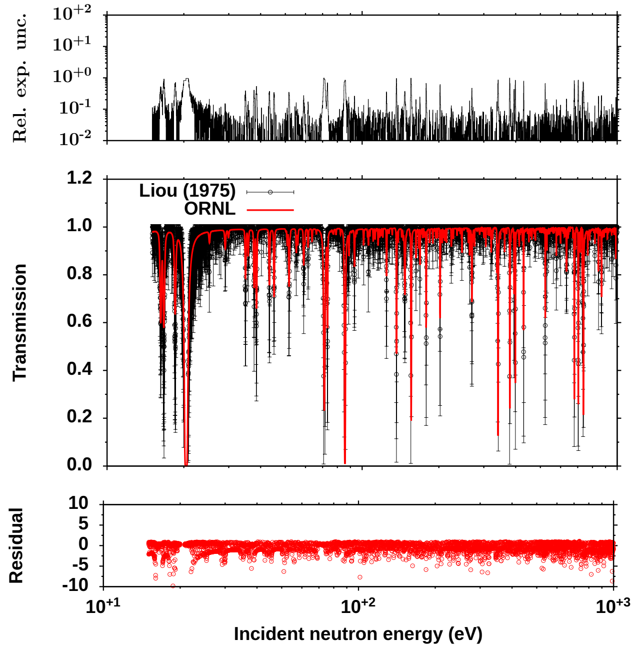

Figure 5. n+^{160}Dy Liou's transmission data measured in the neutron energy range up to 1 keV (black dots) compared to theoretical data (solid red line). Relative experimental uncertainty (top) and residual (bottom) are shown in black solid lines and red dots, respectively.

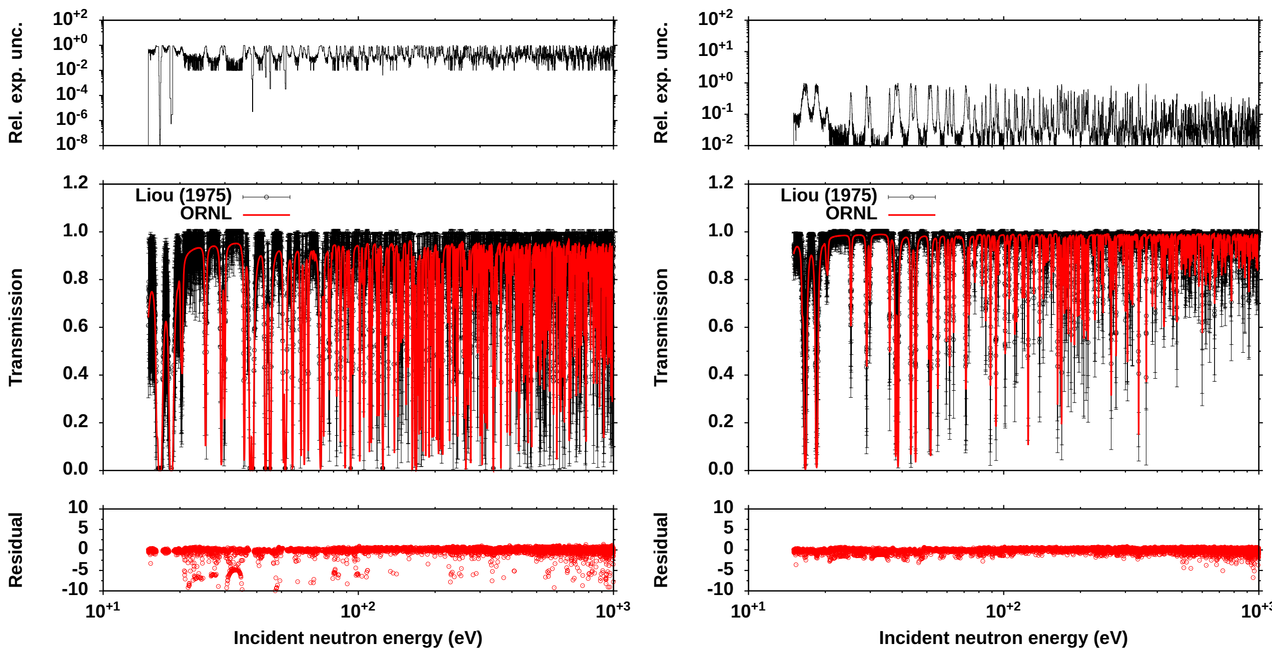

Figure 6. n+^{161}Dy Liou's thick (left) and thin (right) transmission data measured in the neutron energy range up to 1 keV (black dots) compared to theoretical data (solid red line). Relative experimental uncertainty (top) and residual (bottom) are shown in black solid lines and red dots, respectively.

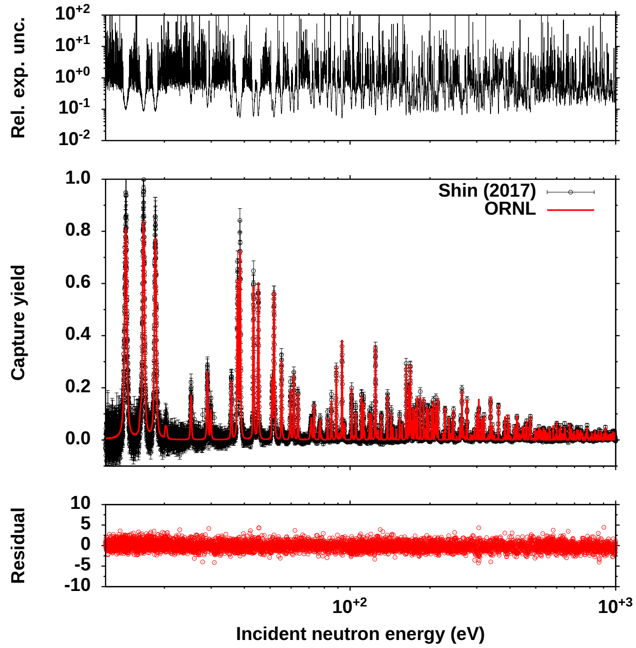

Figure 7. n+^{161}Dy capture yield measured in epithermal energy range at the RPI facility (black dots) compared to theoretical data (solid red line). Relative experimental uncertainty (top) and residual (bottom) are shown in black solid lines and red dots, respectively.

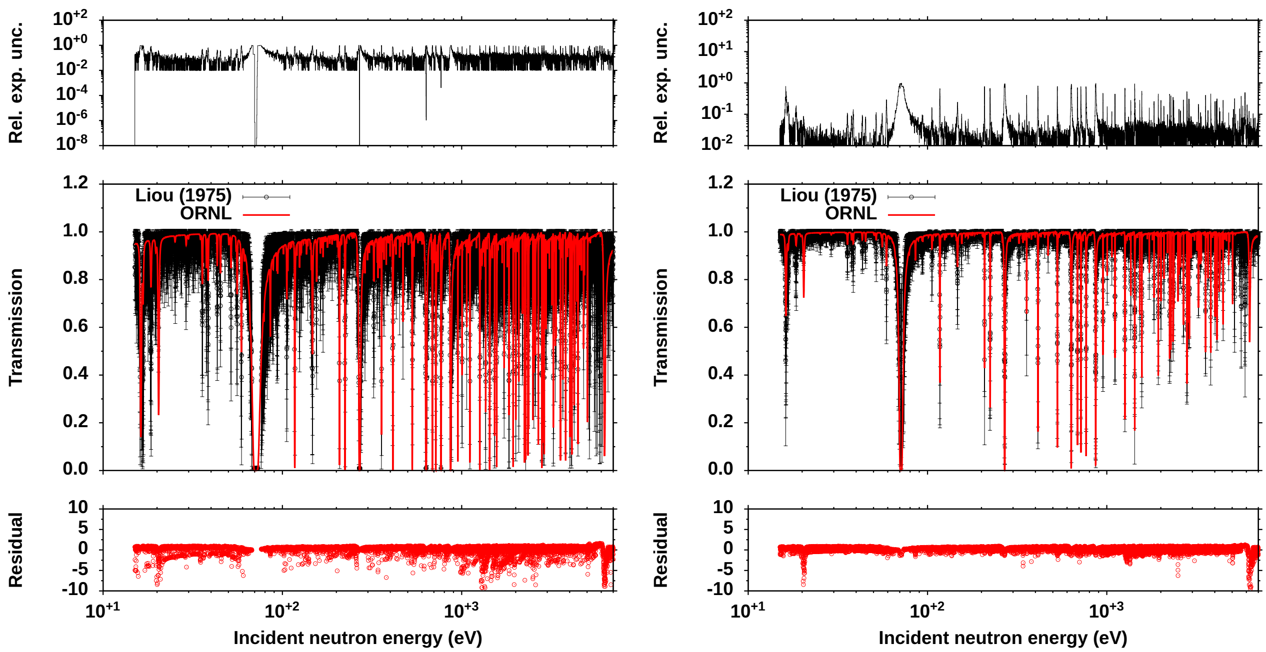

Figure 8. n+^{162}Dy Liou's thick (left) and thin (right) transmission data measured in the neutron energy range up to 1 keV (black dots) compared to theoretical data (solid red line). Relative experimental uncertainty (top) and residual (bottom) are shown in black solid lines and red dots, respectively.

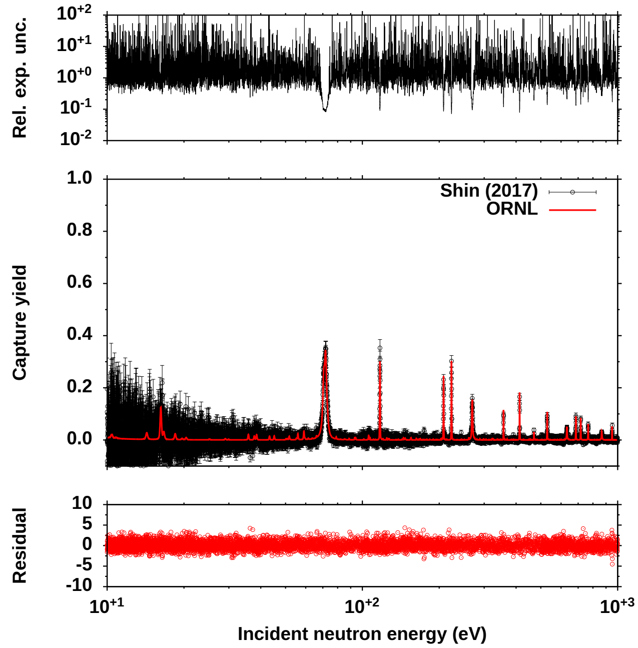

Figure 9. n+^{162}Dy capture yield measured in epithermal energy range at the RPI facility (black dots) compared to theoretical data (solid red line). Relative experimental uncertainty (top) and residual (bottom) are shown in black solid lines and red dots, respectively.

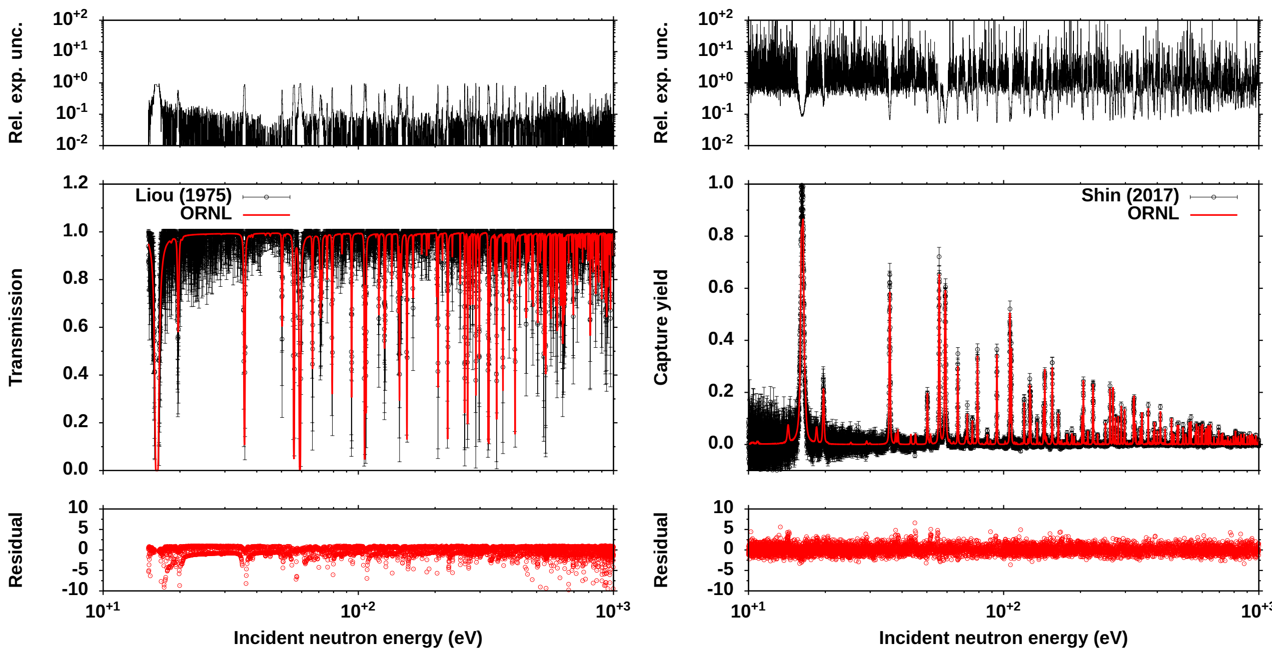

Figure 10. n+^{163}Dy Liou's transmission and Shin's capture data measured in the neutron energy range up to 1 keV (black dots) compared to theoretical data (solid red line). Relative experimental uncertainty (top) and residual (bottom) are shown in black solid lines and red dots, respectively.

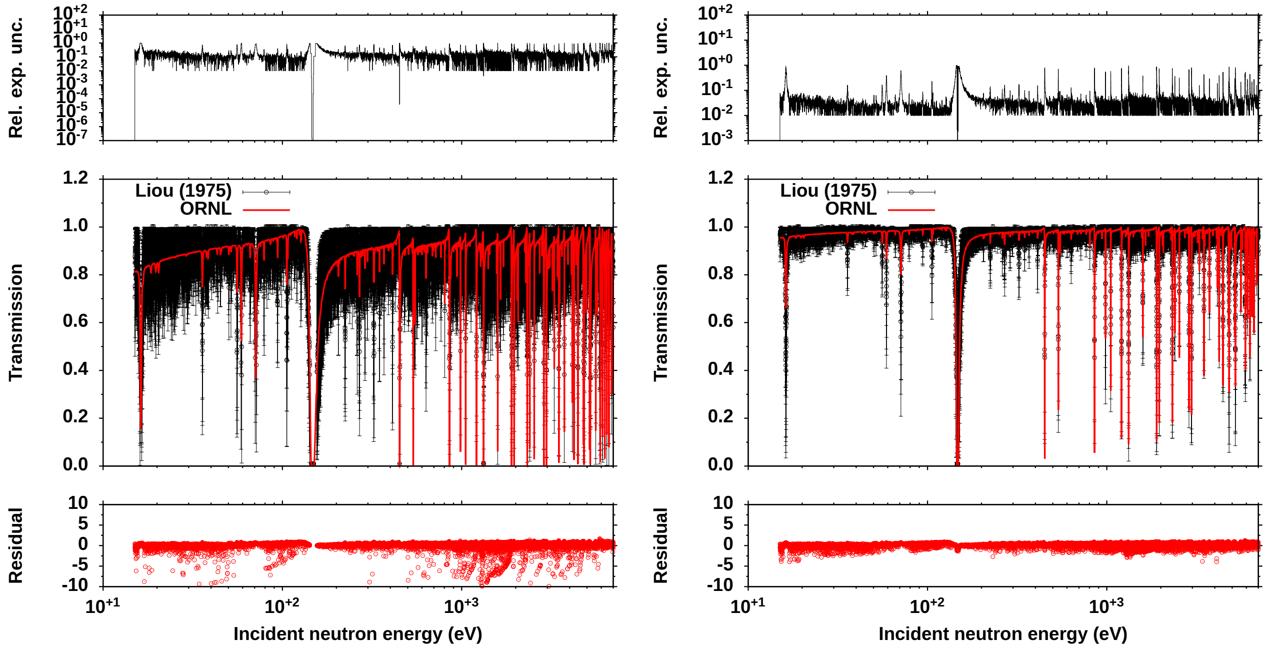

Figure 11. n+^{164}Dy Liou's thick (left) and thin (right) transmission data measured in the neutron energy range up to 1 keV (black dots) compared to theoretical data (solid red line). Relative experimental uncertainty (top) and residual (bottom) are shown in black solid lines and red dots, respectively.

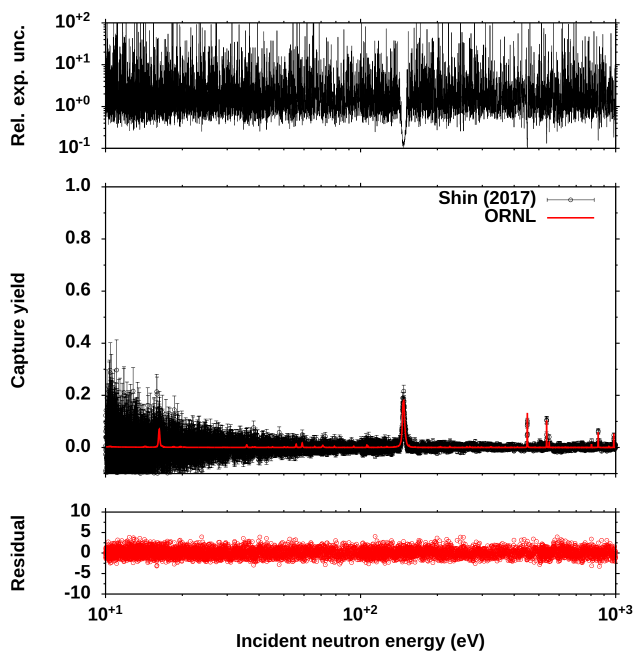

Figure 12. n+^{164}Dy capture yield measured in epithermal energy range at the RPI facility (black dots) compared to theoretical data (solid red line). Relative experimental uncertainty (top) and residual (bottom) are shown in black solid lines and red dots, respectively.

current recommendations to avoid the submittal of ENDF files for natural nuclei, seven RPC matrices (one for each isotope) were generated. This was performed by extracting from the full RPC matrix the sub-matrix corresponding to the specific isotope and stored in a ENDF-formatted file with LRF=3 and LCOMP=1 options. Clearly, this procedure disregards the possible isotope–isotope correlations arising primarily by the fit of experimental data measured on ^{nat}Dy samples. For simplicity but also clarity, the cross section uncertainties and related correlation matrices calculated for the single-isotope RPC for all available reaction channels of each isotope are reported in a group representation averaged over 189 energy bins as shown in Figs. 13–19. Except for two minor isotopes ^{156,158}Dy and ^{162}Dy, the evaluated cross sections feature an uncertainty from about 0.5% to approximately 1–2% in the thermal energy range up to about a few eVs[†]. This relatively low uncertainty is driven by the very low uncertainty ($\ll$ 1%) reported by the measurements on natural samples as shown in Fig. 3. In the same energy region, the correlations are generally 100% because of the strong correlations of resonance parameters for negative levels usually associated with large neutron widths. Above a few eVs, the cross section uncertainties range between 1 and 10%, with mostly short-range positive and negative correlations. The plots also show the cross-reaction correlation matrix of the elastic and capture channels that is generally populated by large portions of negative correlations indicating anti-correlations between the two reaction channels.

[†] To ensure that the cross section uncertainties were not below 0.1%, a multiplication factor was applied to two isotopes, ^{161,164}Dy, over a short energy range. The energy-dependent uncertainty file as implemented in the SAMMY code is shown in Fig. 44

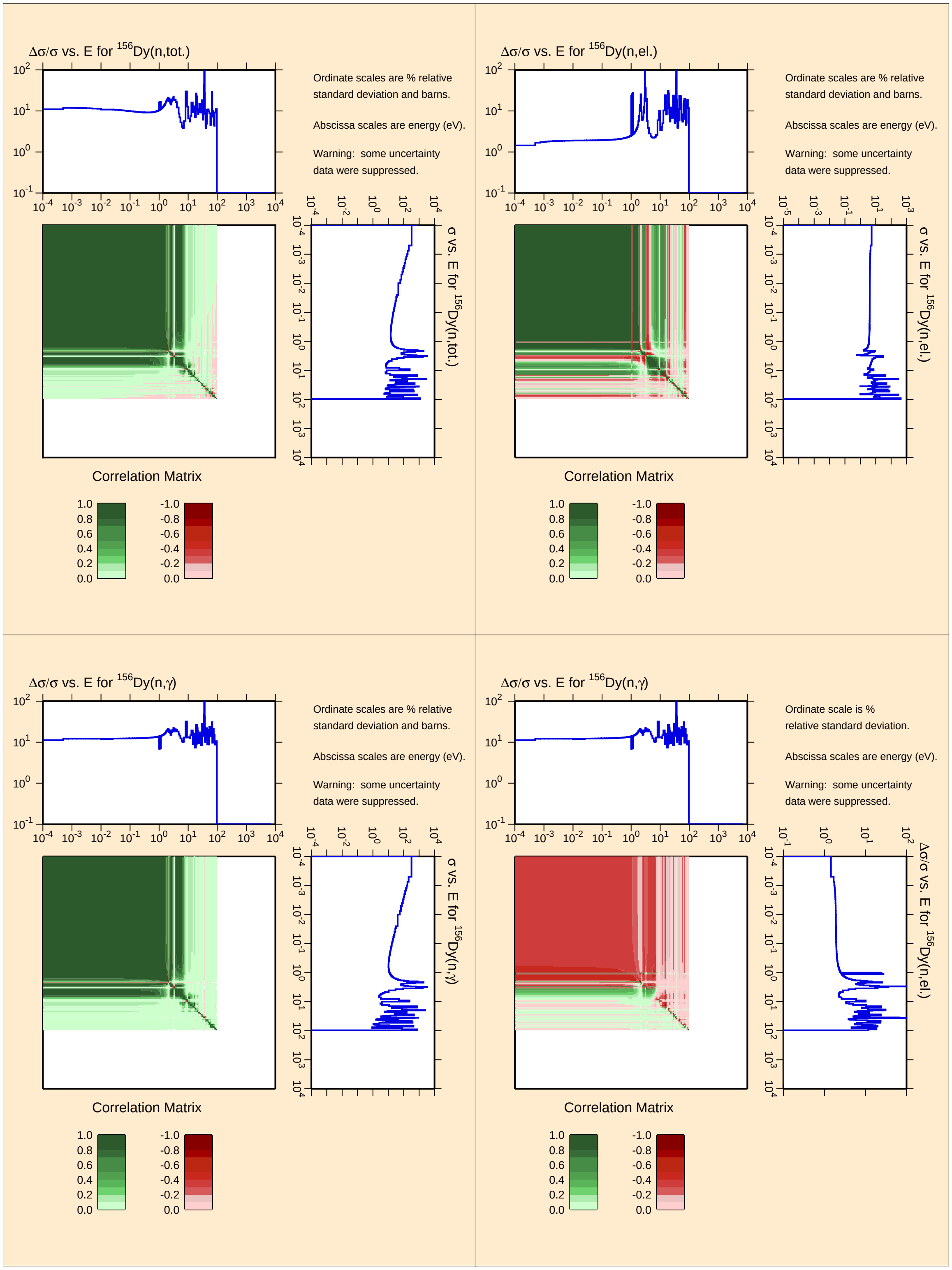

Figure 13. 189-group representation of ^{156}Dy cross sections and related correlation matrices for total, elastic, and capture reaction channels.

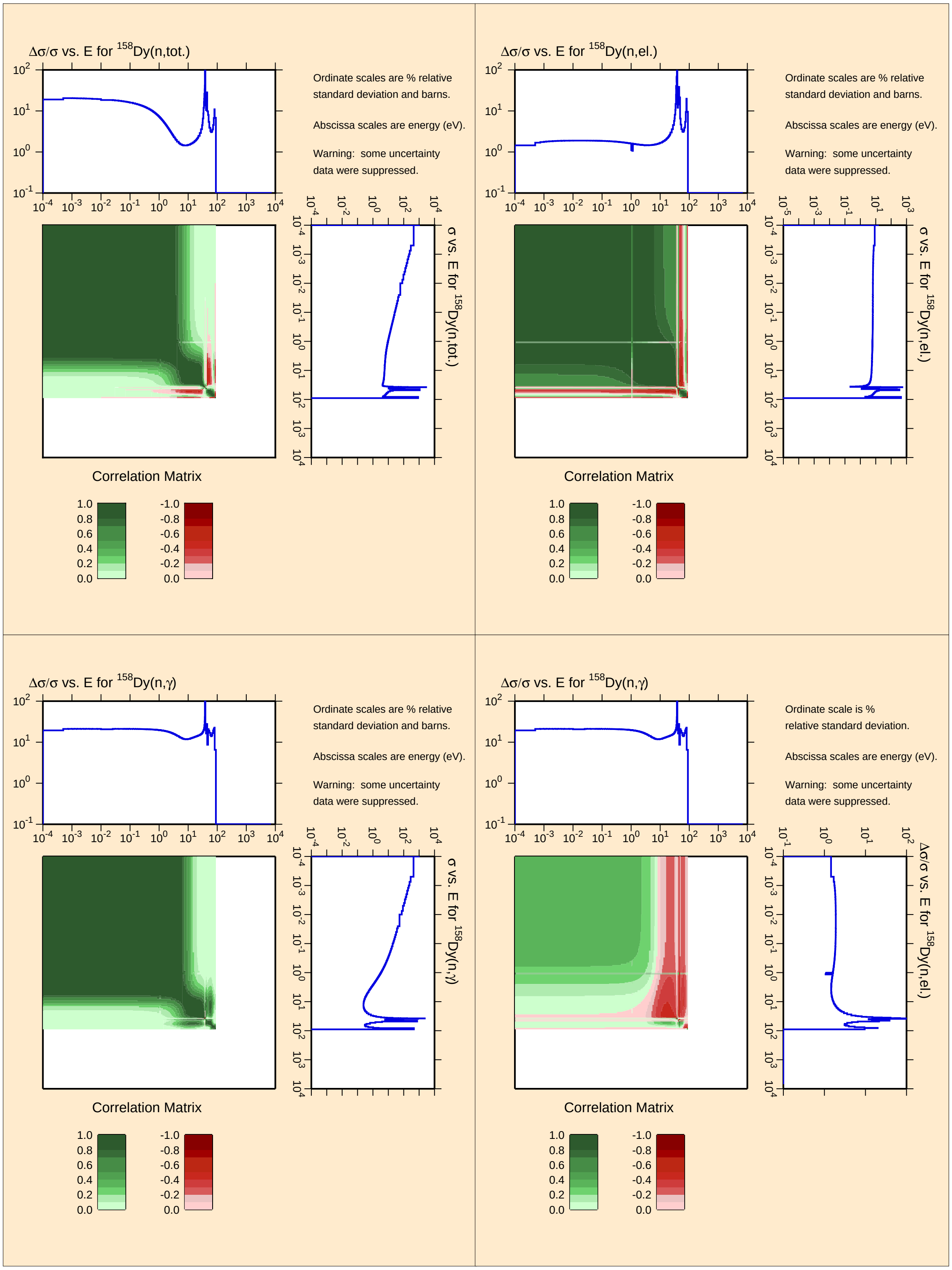

Figure 14. 189-group representation of ^{158}Dy cross sections and related correlation matrices for total, elastic, and capture reaction channels.

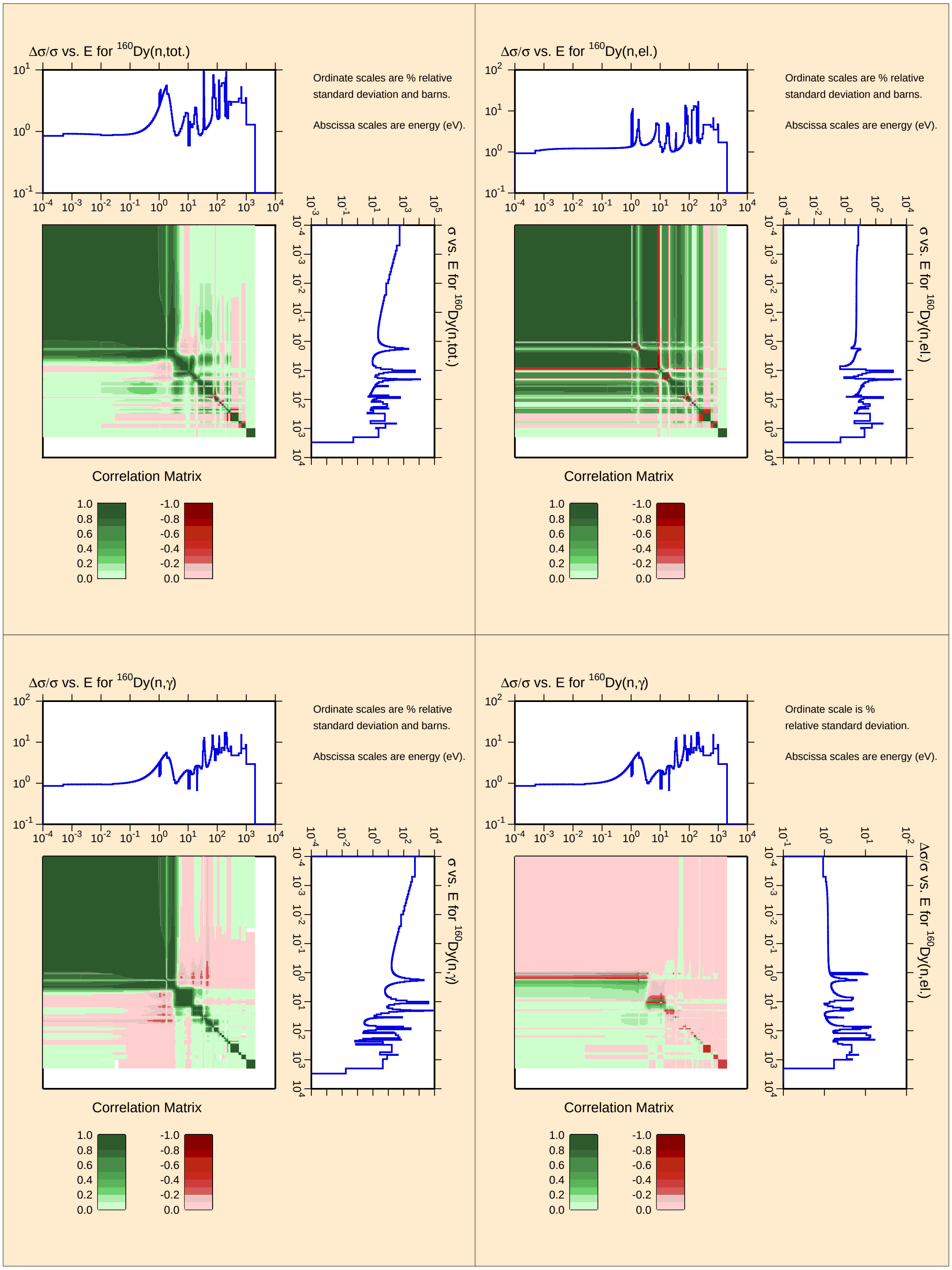

Figure 15. 189-group representation of ^{160}Dy cross sections and related correlation matrices for total, elastic, and capture reaction channels.

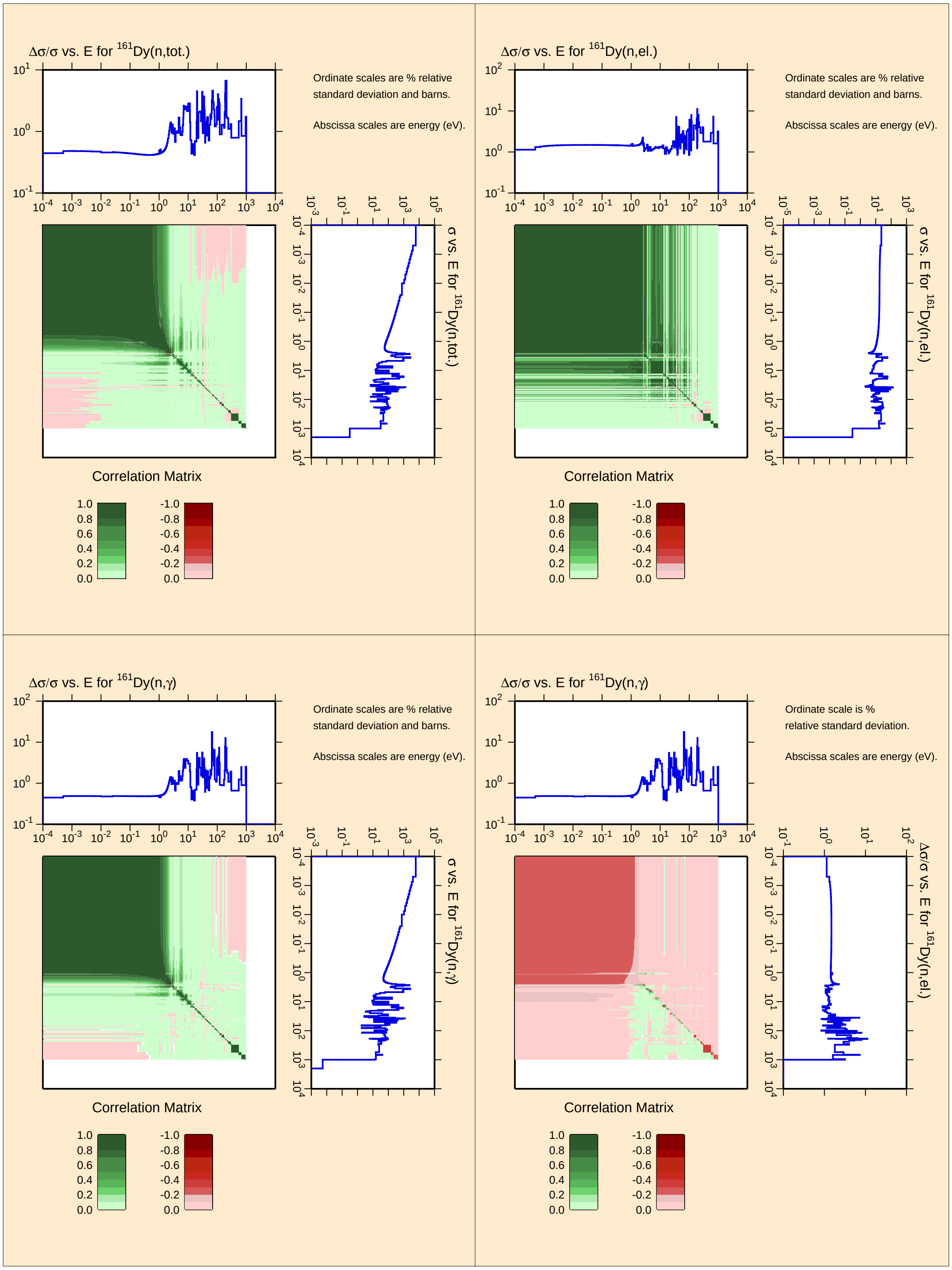

Figure 16. 189-group representation of ^{161}Dy cross sections and related correlation matrices for total, elastic, and capture reaction channels.

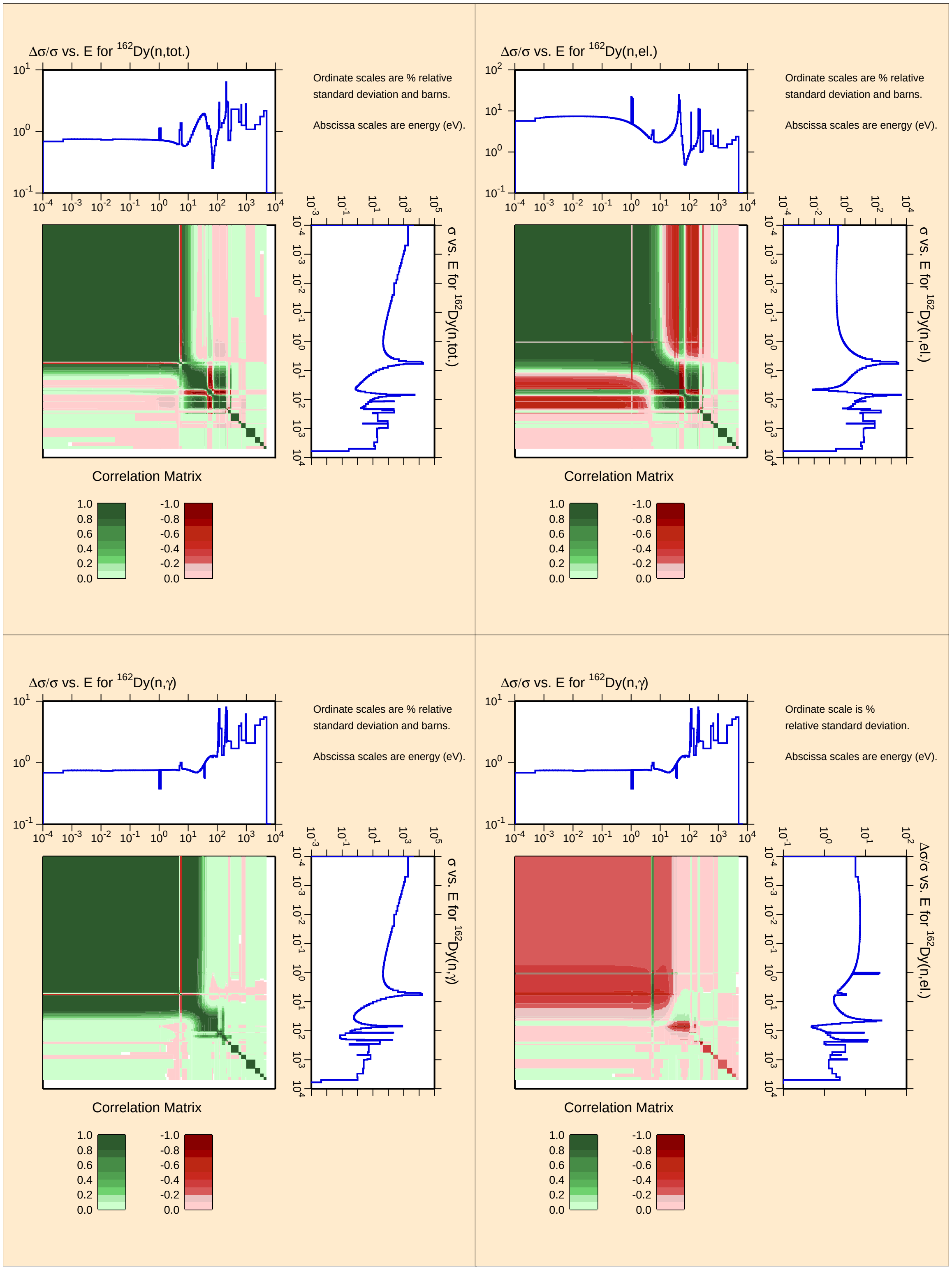

Figure 17. 189-group representation of ^{162}Dy cross sections and related correlation matrices for total, elastic, and capture reaction channels.

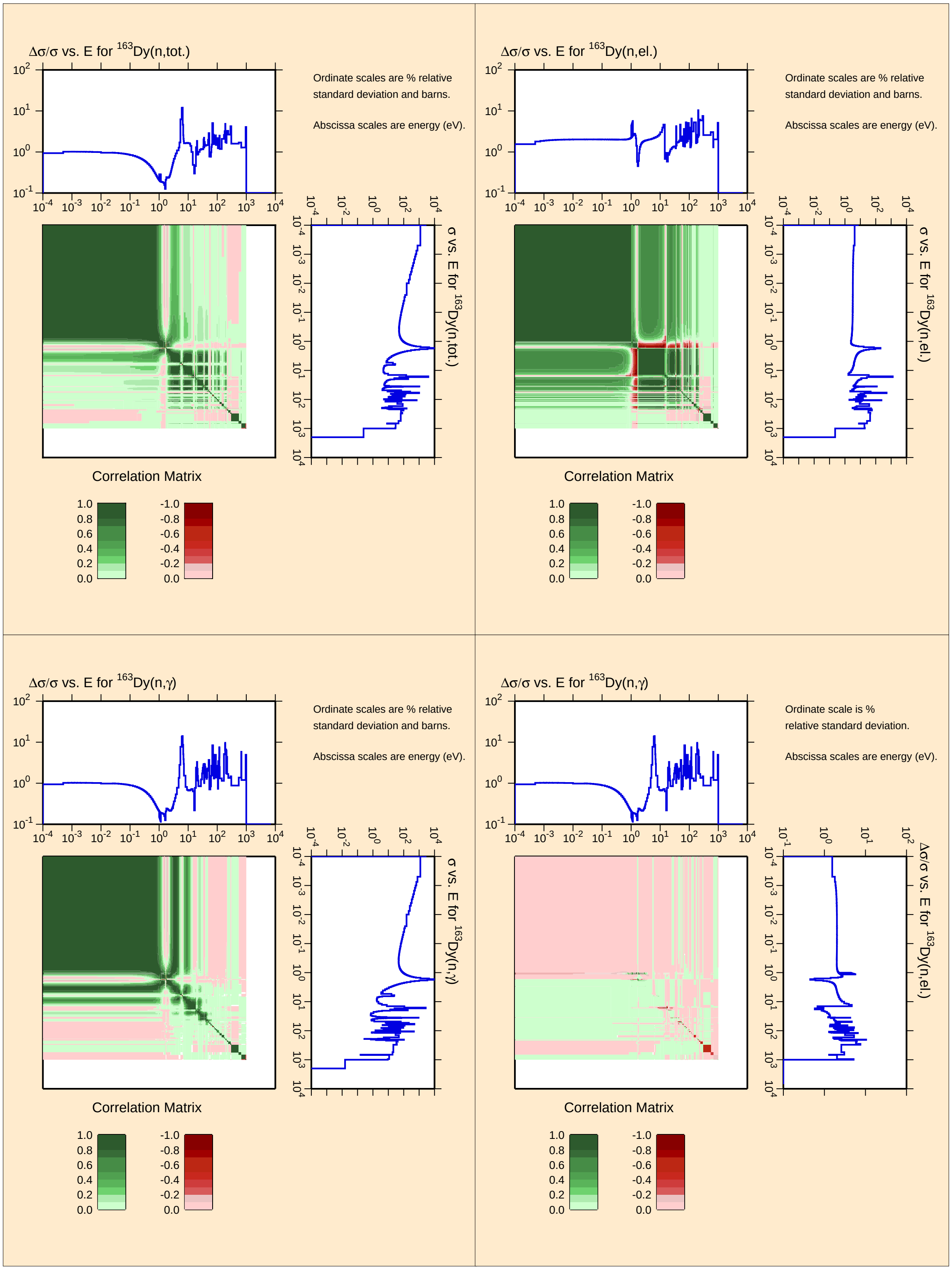

Figure 18. 189-group representation of ^{163}Dy cross sections and related correlation matrices for total, elastic, and capture reaction channels.

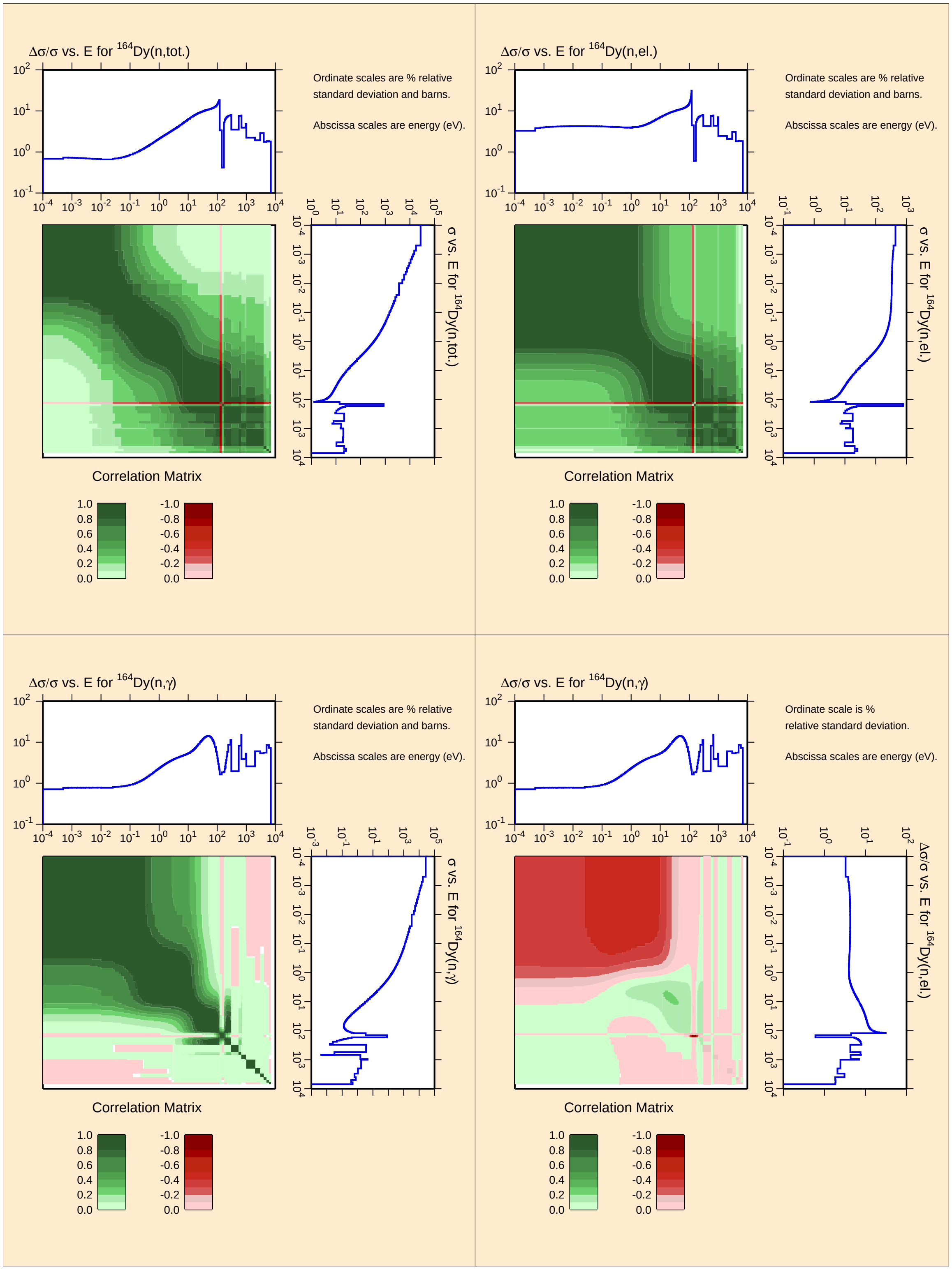

Figure 19. 189-group representation of ^{164}Dy cross sections and related correlation matrices for total, elastic, and capture reaction channels.

5. STATISTICAL PROPERTY OF THE RESONANCE PARAMETERS

The statistical analysis of the resonance parameters can be seen as a test to verify the nuclear reaction theory concerning the Wigner distribution for the level spacings, the Porter–Thomas distribution for the reaction widths, and related reaction channel multiplicity. Therefore, in addition to presenting our results for the observed neutron resonance energies, E, neutron and capture widths, $\Gamma^J_{\rm n}$ and Γ^J_γ, respectively, it is useful to report the study of their statistical properties, such as level spacing systematics and strength functions (or corresponding pole strength). In Figs. 20–26, cumulative plots of the number of observed s-wave vs energy for seven isotopes, $^{156,158,160\text{-}164}$Dy, are displayed with the estimated average level spacings and strength functions. These values were calculated from the fit of the observed energy levels and neutron widths over the entire positive energy range, although the choice of the upper energy in the fit can clearly impact the fitted values of the level spacing $\langle D_0\rangle$ and strength function $\langle S_0\rangle$ (or pole strength $\langle s_0\rangle$). The estimate of the average s-level spacing $\langle D_0\rangle$ reported in the figures was obtained as the inverse of the slope of a straight line fitted to the observed energy levels as

$$\frac{1}{\langle D_0\rangle} = \frac{\lambda}{\Delta E_\lambda}\,, \tag{10}$$

where $\Delta E_\lambda = \lambda(E_\lambda - E_1)/(\lambda-1)$ and $\lambda > 1$ is the energy level index for monotonically increasing positive energies whose upper limit is the total number of s-levels $\Lambda \equiv \sup\{\lambda\}$. For the strength function, the following relation was used:

$$S_l\,\Delta E_\Lambda = \sum_{\lambda>1}^{\Lambda} g_\lambda \Gamma^{0J(l)}_{n\lambda} v_l/(2l+1)\,, \tag{11}$$

where $\Gamma^{0J(l)}_{n\lambda} = \Gamma^{J(l)}_{n\lambda}/\sqrt{1\text{eV}/E_\lambda}$ is the reduced width and $v_l = \rho/P_l$ with $\rho = kR$ and $P_l \equiv P_l(\rho)$ is the penetrability factor. For s-wave, v_l is clearly unitary because $P_0 = \rho$.

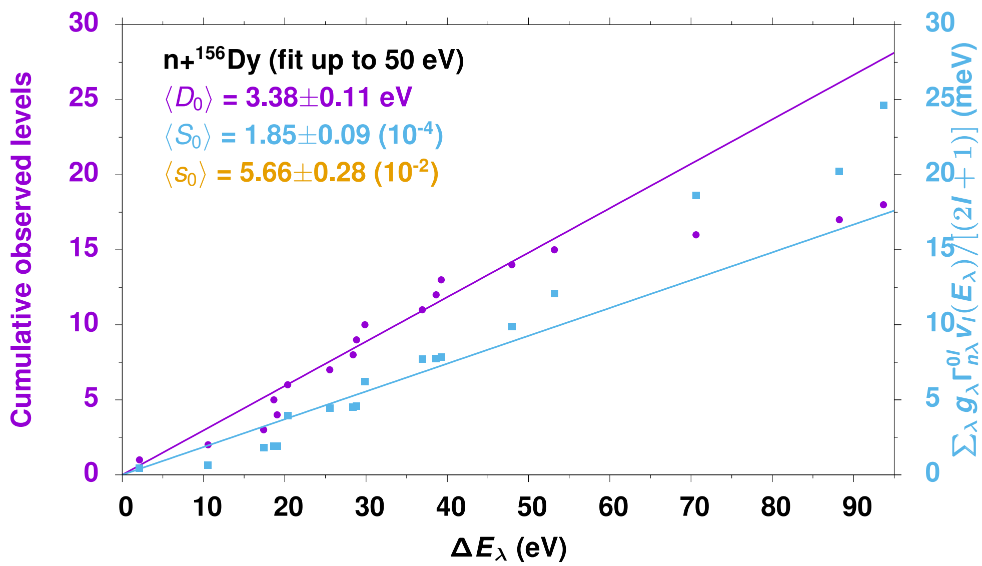

Figure 20. Plot of the cumulative number of observed s-wave (purple dots) vs energy for n+^{156}Dy. The values of average s-level spacings $\langle D_0\rangle$ shown in the plot represent the inverse of the slope of a straight line fitted to the data (purple and blue lines) up to 50 eV. In blue, the fit of the neutron strength function S_0 is also shown together with the value of the related pole strength s_0 (in yellow).

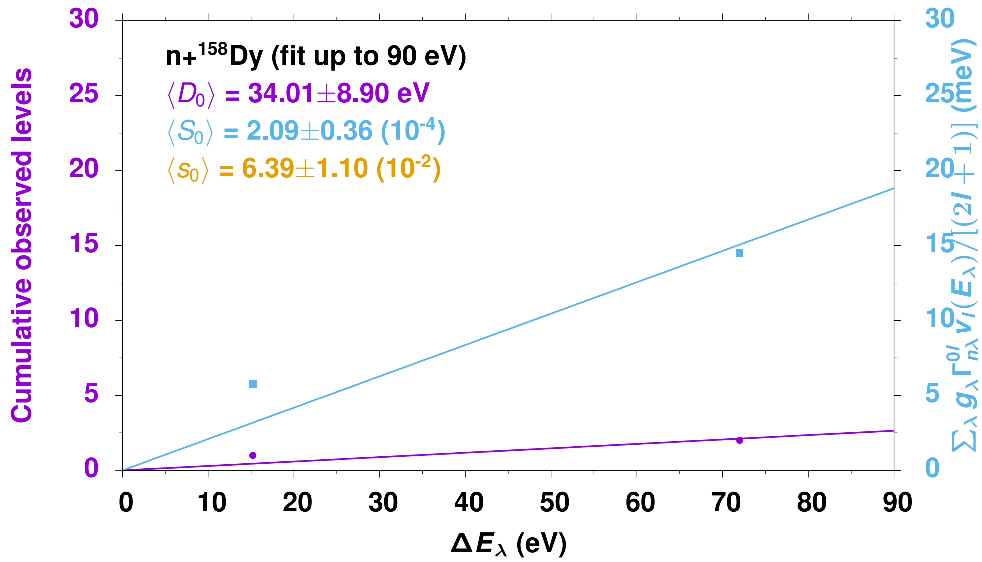

Figure 21. Plot of the cumulative number of observed s-wave (purple dots) vs energy for n+^{158}Dy. The values of average s-level spacings $\langle D_0 \rangle$ shown in the plot represent the inverse of the slope of a straight line fitted to the data (purple and blue lines) up to 90 eV. In blue, the fit of the neutron strength function S_0 is also shown together with the value of the related pole strength s_0 (in yellow).

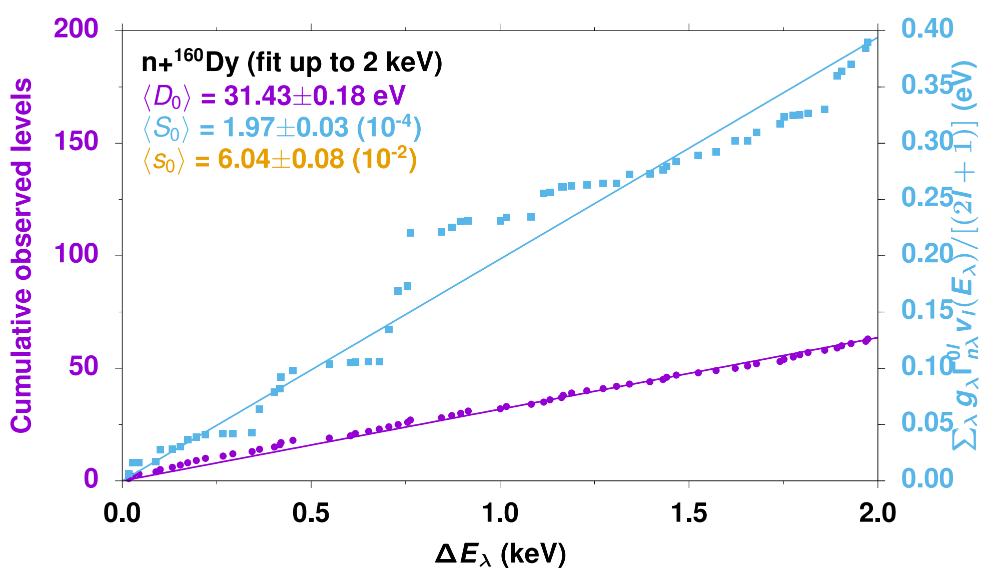

Figure 22. Plot of the cumulative number of observed s-wave (purple dots) vs energy for n+^{160}Dy. The values of average s-level spacings $\langle D_0 \rangle$ shown in the plot represent the inverse of the slope of a straight line fitted to the data (purple and blue lines) up to 90 eV. In blue, the fit of the neutron strength function S_0 is also shown together with the value of the related pole strength s_0 (in yellow).

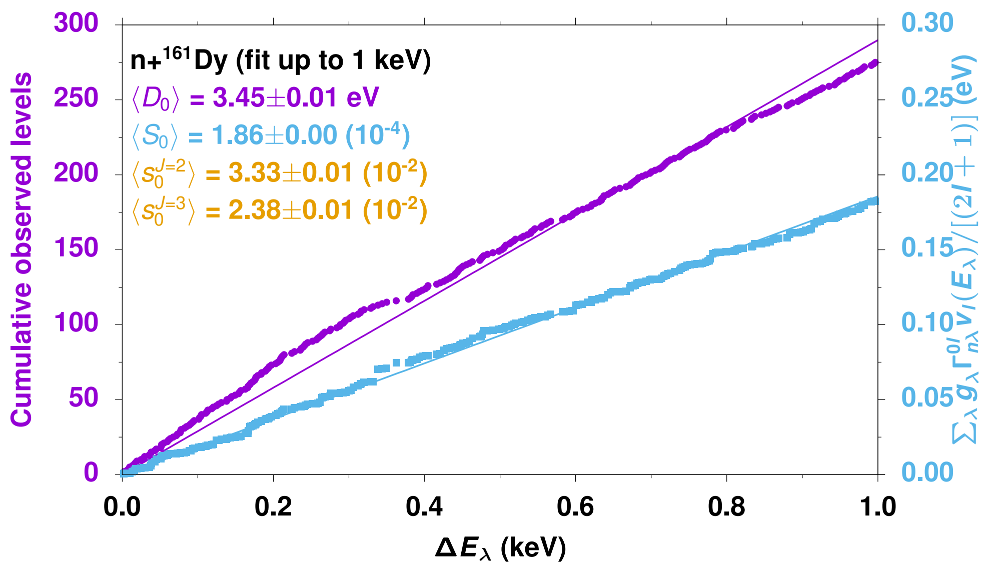

Figure 23. Plot of the cumulative number of observed s-wave (purple dots) vs energy for n+^{161}Dy. The values of average s-level spacings $\langle D_0 \rangle$ shown in the plot represent the inverse of the slope of a straight line fitted to the data (purple and blue lines) up to 1 keV. In blue, the fit of the neutron strength function S_0 is also shown together with the value of the related pole strength s_0 (in yellow).

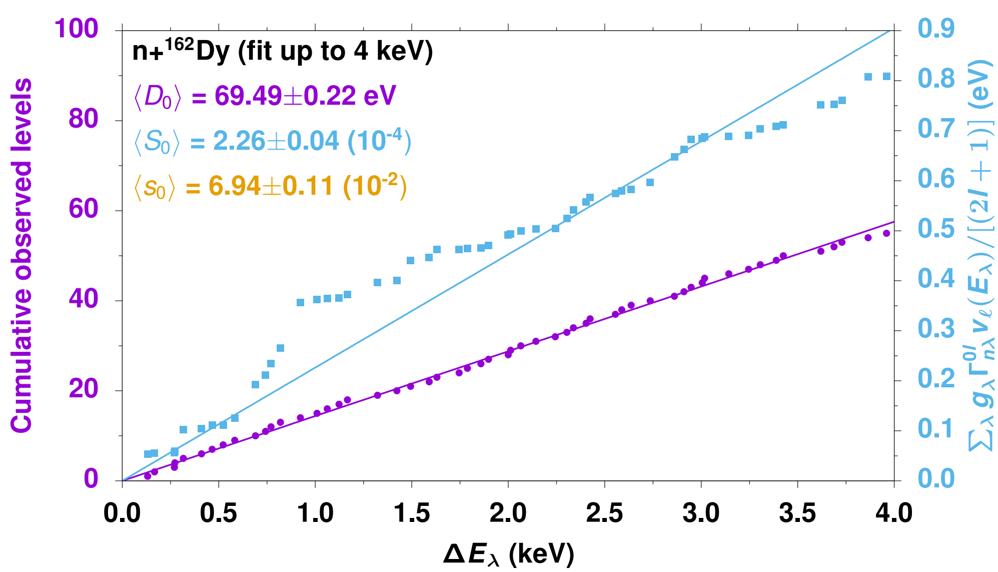

Figure 24. Plot of the cumulative number of observed s-wave (purple dots) vs energy for n+^{162}Dy. The values of average s-level spacings $\langle D_0 \rangle$ shown in the plot represent the inverse of the slope of a straight line fitted to the data (purple and blue lines) up to 5 keV. In blue, the fit of the neutron strength function S_0 is also shown together with the value of the related pole strength s_0 (in yellow).

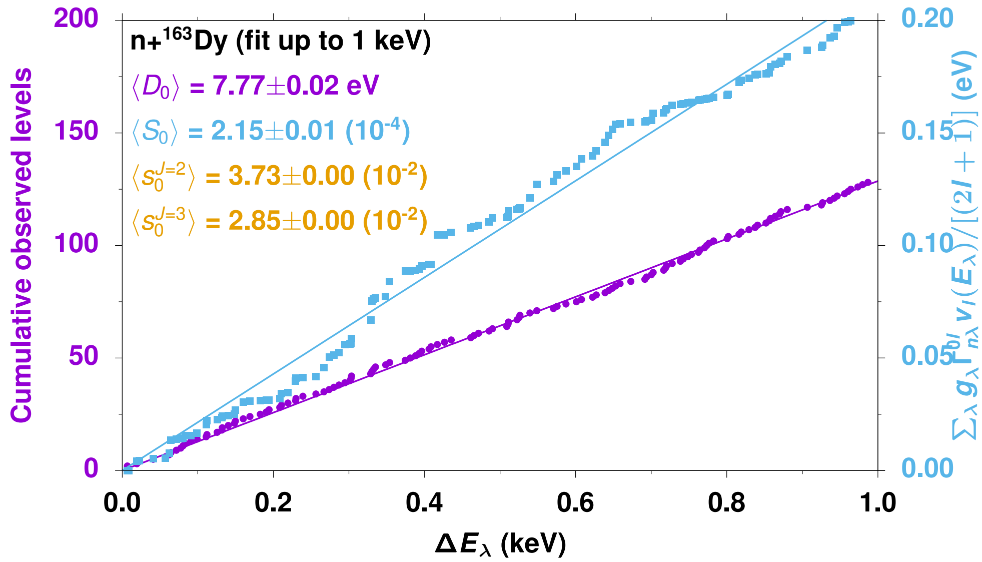

Figure 25. Plot of the cumulative number of observed s-wave (purple dots) vs energy for n+^{163}Dy. The values of average s-level spacings $\langle D_0 \rangle$ shown in the plot represent the inverse of the slope of a straight line fitted to the data (purple and blue lines) up to 1 keV. In blue, the fit of the neutron strength function S_0 is also shown together with the value of the related pole strength s_0 (in yellow).

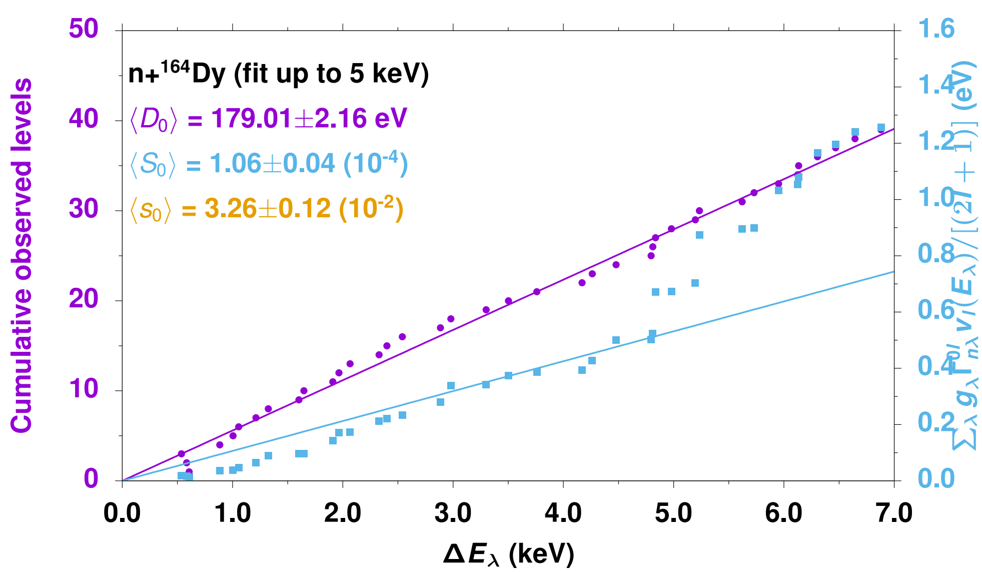

Figure 26. Plot of the cumulative number of observed s-wave (purple dots) vs energy for n+^{164}Dy. The values of average s-level spacings $\langle D_0 \rangle$ shown in the plot represent the inverse of the slope of a straight line fitted to the data (purple and blue lines) up to 7 keV. In blue, the fit of the neutron strength function S_0 is also shown together with the value of the related pole strength s_0 (in yellow).

6. REPOSITORY

The set of directories and related files used to generate the set of Dy evaluations has been stored in a GitHub repository found at the following link `https://code-int.ornl.gov/xtp/dysprosium`‡. When possible, the structure of the repository is designed to have a set of directories following the logical steps of the evaluation procedure. Each directory contains the files, scripts, and subdirectories necessary to reproduce the files submitted to ENDF repository. These folders are briefly described below and reported in such a way that roughly reproduces the execution order.

- `parameter` contains different versions of parameter files with a name convention **`dy-ver.par`**, where **`ver`** is the version label—for instance, **`endf`**, **`beta1`**, **`final`**. In addition to the resonance parameters (level energies, channel radii and widths), the files are set up to contain quantum number information and related particle pairs for seven Dy isotopes. As explained later, the isotopic abundance of each isotope is specified in the input files together with other experimental corrections.
    - `geraspin` is designed to generate the quantum number information as reported in the parameter files above. This is performed by running the **`dy.csh`** script, which uses existing input files for the SAMQUA code of the type **`dy-wave.inp`**, where **`wave`** is the input variable of the script and refers to the number of partial waves setup for each input file. The file **`masses.gp`** uses GNUPLOT to print the isotope masses as reported in the parameter files.
    - `coher` computes thermal properties such as thermal cross sections and scattering lengths as reported in Table 5 for each isotope from a specific **`dy-ver.par`** file.
    - `stat` generates plots of the statistical properties of the resonance parameters from a specific **`dy-ver.par`** file by using GNUPLOT after running the SAMDIST code. This is performed by running the **`run_stat.csh`** script with **`ver`** as input variable. Assumptions on spin group numbers listed in the parameter file are made. Based on these, the input files to run the SAMDIST code are automatically generated in **`testdist.csh`**. The script **`stat.csh`** uses files with extension **`gp`** to generate plots of resonance parameter statistical properties from a specific parameter file.
- `exfor` contains the measured data files with extension **`exf`** retrieved from the EXFOR library. These are used to generate input files for SAMMY with extension **`twenty`**. The files with extension **`exf`** and **`twenty`** contain the same information except for minor changes like negative values for the data type such as cross section and neutron capture yield, or inclusion of data uncertainty if not explicitly given in the EXFOR library.
    - The subdirectory `crunch` contains the plots for the crunch tables generated by the GNUPLOT script **`crunch.gp`**, which reads the measured data files. The derived crunch tables are the same used in the SAMMY input files.
- `inputs` contains the SAMMY inputs corresponding to each experiments. These files are set up with alpha-numeric cards to solely contain parameters of the experimental configurations. The quantum-number information, i.e., particle pair definitions with related channel spins and radii, are included in the parameter file in the `parameter` directory.

‡Available only internally for ORNL users.

- `thermal` is a directory containing data files in **`twenty`** stored in the subdirectory `data` and referring to different compilation of thermal values for each Dy isotope.
- `runs` is defined to calculate cross section or yield data for a set of measured data listed in the script **`sammy.csh`**. The data are reconstructed for a specific parameter **`ver`** found in the script.
- `cov` contains scripts to both perform the fit of selected measured data and generate ENDF-formatted file 2 and 32 for each isotope to be used in the final assembly of the ENDF file. The resonance parameter information and associated covariance matrix is extracted from the `SAMMY.COV` binary file which a multi-isotope covariance matrix obtained by the global fit of seven Dy isotopes.
- `dy1[**]` are directories containing `SAMMY.LPT` and `SAMMY.LST` files for a specific set of resonance parameters.
- `ndf` is a directory for the generation of a set of ENDF files for each Dy isotope with minimal information for cross section and covariance processing purposes. The information includes MF=2 and MF=32 sections starting from a parameter file **`dy-ver.par`** stored in the `parameter` directory. The ENDF file includes a section for MF=3 and MF=33 with zeros to allow processing with a code such as NJOY. The script to generate and process minimal ENDF files including only cross section information such as MF=2 and MF=3 sections for each Dy isotope is **`ndf.csh`**. The input parameter of this script is the specific parameter version **`ver`**. The script **`ndf_cov.csh`** is used similarly to **`ndf.csh`** but designed to include information for MF=32 and MF=33 sections in the ENDF file to quantify processed cross section covariances as well. The processing is performed by calling the script **`xcs-res.constE-dy.csh`**.
- `report` is a directory storing the files and figures used to generate the present ORNL/TM report.
- `nndc` contains the final ENDF-formatted files, **`n-066_Dy_iso.endf`**, submitted to the National Nuclear Data Center.

7. CONCLUSIONS

The set of the RM parameters for neutron-induced resonances of seven Dy isotopes, $^{156,158,160-164}$Dy, in the incident energy range from thermal to several keVs was generated by applying the SAMMY evaluation procedure. The multi-level multi-channel *R*-matrix shape fitting analysis was performed on available experimental data for natural capture yield and transmission data as well as isotopically enriched capture yield data. Experimental conditions such as resolution function, finite size sample, detector efficiencies, and nuclide abundances of sample, multiple scattering, self-shielding, normalization, background, and Doppler broadening were taken into account.

In addition to the guidance provided by Sears' (or NIST) compilation [12] for the thermal constants, the experimental database in the thermal and low-energy region up to 15 eV consisted of both high-resolution capture yields and transmission data [7]. Due to their extension to thermal energies, these data were extremely relevant in the resonance parameter evaluation. In this region, the evaluated thermal scattering and capture constant for the ^{164}Dy isotope shows differences with NIST compilation up to 8%. Also for ^{161}Dy isotopes, this work reports a value of the scattering cross section 10% higher than the NIST's reported value but in agreement with other evaluated works [6]. Particular emphasis should be devoted in future experimental campaigns to measuring scattering lengths for these two isotopes, particularly for the most abundant isotope, ^{164}Dy, with the largest total thermal cross section among the seven Dy isotopes. Moreover, future evaluation works should develop the capability to include scattering lengths in the fitting procedure, among other possible measured quantities. Uncertainty quantification of the total, elastic scattering, and capture cross section for all isotopes has been reported, for convenience, in 189-group representation as shown in Figs. 13–19. The uncertainty in the thermal energy region were about 1% constrained by the transmission, and capture measurements on natural samples [7] were reported to have a similar uncertainty.

In the energy region above 15 eV, although high-resolution capture yield data [8] are available, high-resolution transmission data are still needed for isotopically enriched samples. The currently available Liou's transmission data [5] are poorly documented in the uncertainty quantification analysis, and it seems very likely that the reported data communicated to the EXFOR database are not measured data but total cross section data reconstructed from resonance parameters fitted to the measured transmission data. Moreover, Liou's measurements campaign included capture measurements that are not available in the EXFOR library. The lack of modern transmission data measured on isotopically enriched samples in the neutron energy above 15 eV also precludes any attempt to extend the RRR to the currently reported upper energy ranges.

Integral benchmarks reporting reactivity coefficients such as k_{eff} are usually used to validate underlying nuclear data for a given configuration of materials—including fissile actinides and other chosen nuclei —for instance, to test their natural propensity to absorb neutrons. Reactivity coefficients of interest for criticality safety applications can be, by design, very sensitive to the thermal and epithermal region up to a few eVs. Therefore, the present evaluation based on Block's recent transmission data (measured from thermal up to 15 eV) represents a perfect example of nuclear data ready for validation purposes. However, in the specific case of Dy isotopes, there is a very limited number of modern benchmarks that can be used to perform a conclusive validation over a comprehensive suite of cases. Therefore, no particular validation test was performed on the evaluated data presented in this work.

Finally, this work represents one of the first attempts to generate a fully reproducible evaluation in the RRR as this is the primary goal of the Working Party on International Nuclear Data Evaluation Co-operation Subgroup 49.

REFERENCES

[1] D.A. Brown, M.B. Chadwick, R. Capote, A.C. Kahler, A. Trkov, M.W. Herman, A.A. Sonzogni, Y. Danon, A.D. Carlson, M. Dunn, D.L. Smith, G.M. Hale, G. Arbanas, R. Arcilla, C.R. Bates, B. Beck, B. Becker, F. Brown, R.J. Casperson, J. Conlin, D.E. Cullen, M.-A. Descalle, R. Firestone, T. Gaines, K.H. Guber, A.I. Hawari, J. Holmes, T.D. Johnson, T. Kawano, B.C. Kiedrowski, A.J. Koning, S. Kopecky, L. Leal, J.P. Lestone, C. Lubitz, J.I. Márquez Damián, C.M. Mattoon, E.A. McCutchan, S. Mughabghab, P. Navratil, D. Neudecker, G.P.A. Nobre, G. Noguere, M. Paris, M.T. Pigni, A.J. Plompen, B. Pritychenko, V.G. Pronyaev, D. Roubtsov, D. Rochman, P. Romano, P. Schillebeeckx, S. Simakov, M. Sin, I. Sirakov, B. Sleaford, V. Sobes, E.S. Soukhovitskii, I. Stetcu, P. Talou, I. Thompson, S. van der Marck, L. Welser-Sherrill, D. Wiarda, M. White, J.L. Wormald, R.Q. Wright, M. Zerkle, G. Žerovnik, and Y. Zhu. ENDF/B-VIII.0: The 8$^{\text{th}}$ Major Release of the Nuclear Reaction Data Library with CIELO-project Cross Sections, New Standards and Thermal Scattering Data. *Nuclear Data Sheets*, 148:1 – 142, 2018. Special Issue on Nuclear Reaction Data.

[2] M.B. Chadwick, P. Obložinský, M. Herman, N.M. Greene, R.D. McKnight, D.L. Smith, P.G. Young, R.E. MacFarlane, G.M. Hale, S.C. Frankle, A.C. Kahler, T. Kawano, R.C. Little, D.G. Madland, P. Moller, R.D. Mosteller, P.R. Page, P. Talou, H. Trellue, M.C. White, W.B. Wilson, R. Arcilla, C.L. Dunford, S.F. Mughabghab, B. Pritychenko, D. Rochman, A.A. Sonzogni, C.R. Lubitz, T.H. Trumbull, J.P. Weinman, D.A. Brown, D.E. Cullen, D.P. Heinrichs, D.P. McNabb, H. Derrien, M.E. Dunn, N.M. Larson, L.C. Leal, A.D. Carlson, R.C. Block, J.B. Briggs, E.T. Cheng, H.C. Huria, M.L. Zerkle, K.S. Kozier, A. Courcelle, V. Pronyaev, and S.C. van der Marck. ENDF/B-VII.0: Next Generation Evaluated Nuclear Data Library for Nuclear Science and Technology. *Nuclear Data Sheets*, 107(12):2931–3060, 2006. Evaluated Nuclear Data File ENDF/B-VII.0.

[3] M.B. Chadwick, M. Herman, P. Obložinský, M.E. Dunn, Y. Danon, A.C. Kahler, D.L. Smith, B. Pritychenko, G. Arbanas, R. Arcilla, R. Brewer, D.A. Brown, R. Capote, A.D. Carlson, Y.S. Cho, H. Derrien, K. Guber, G.M. Hale, S. Hoblit, S. Holloway, T.D. Johnson, T. Kawano, B.C. Kiedrowski, H. Kim, S. Kunieda, N.M. Larson, L. Leal, J.P. Lestone, R.C. Little, E.A. McCutchan, R.E. MacFarlane, M. MacInnes, C.M. Mattoon, R.D. McKnight, S.F. Mughabghab, G.P.A. Nobre, G. Palmiotti, A. Palumbo, M.T. Pigni, V.G. Pronyaev, R.O. Sayer, A.A. Sonzogni, N.C. Summers, P. Talou, I.J. Thompson, A. Trkov, R.L. Vogt, S.C. van der Marck, A. Wallner, M.C. White, D. Wiarda, and P.G. Young. ENDF/B-VII.1 Nuclear Data for Science and Technology: Cross Sections, Covariances, Fission Product Yields and Decay Data. *Nuclear Data Sheets*, 112(12):2887–2996, 2011. Special Issue on ENDF/B-VII.1 Library.

[4] S. F. Mughabghab. *Neutron Cross Sections, Vol. 1, Part B*. Academic Press, 1984.

[5] H. I. Liou, G. Hacken, J. Rainwater, and U. N. Singh. Neutron resonance spectroscopy: The separated isotopes of Dy. *Phys. Rev. C*, 11:462–473, Feb 1975.

[6] Y. D. Lee, S. Y. Oh, and J. H. Chang. Total and Capture Cross Sections of Dysprosium Isotopes up to 20 MeV. *Nuclear Science and Engineering*, 151(3):319–334, 2005.

[7] R.C. Block, M.C. Bishop, D.P. Barry, G. Leinweber, R.V. Ballad, J.A. Burke, M.J. Rapp, Y. Danon, A. Youmans, N.J. Drindak, G.N. Kim, Y.-R. Kang, M.W. Lee, and S. Landsberger. Neutron transmission and capture measurements and analysis of Dy from 0.01 to 550 eV. *Progress in Nuclear Energy*, 94:126–132, 2017.

[8] S. G. Shin, Y. U. Kye, W. Namkung, M. H. Cho, Y.-R. Kang, M. W. Lee, G.N. Kim, T.-I. Ro, Y. Danon, D. Williams, G. Leinweber, R. C. Block, D. P. Barry, and M.J. Rapp. Neutron capture measurements and resonance parameters of dysprosium. *THE EUROPEAN PHYSICAL JOURNAL A*, 53:203–225, 2017.

[9] N. M. Larson. Updated users' guide for SAMMY: Multilevel R-Matrix fits to neutron data using Bayes' equations. Technical Report ORNL/TM-9179/R8, Oak Ridge National Laboratory, 2008.

[10] S. F. Mughabghab. *Atlas of Neutron Resonances: Thermal Cross Sections and Resonance Parameters*. Elsevier, 2006.

[11] Fritz H. Fröhner and Olivier Bouland. Treatment of external levels in neutron resonance fitting: Application to the nonfissile nuclide 52cr. *Nuclear Science and Engineering*, 137(1):70–88, 2001.

[12] V. F. Sears. Neutron scattering lengths and cross sections. *Neutron News*, 3(3):26–37, 1992.

[13] F. Farina Arboccò, P. Vermarcke, K. Smits, L. Sneyers, and K. Stijckmans. Experimental determination of k_0, Q_0 factors, effective resonance energies and neutron cross-sections for 37 isotopes of interest in NAA. *Journal of Radioanalytical and Nuclear Chemistry*, 302:655–672, 2014.

[14] V. P. Vertebny, M. F. Vlasov, N. L. Gnidak, A. L. Kirilyuk, E. A. Pavlenko, M. V. Pasechnik, N. A. Trofimova, and A. F. Fedorov. Neutron cross-sections of the isotopes of ^{161}Dy, ^{162}Dy, ^{163}Dy and ^{164}Dy. Technical Report 31, 1972. USSR report to the I.N.D.C.

[15] Progress Report 11, 1971. Yaderno-Fizicheskie Issledovaniya Reports.

APPENDIX A. SAMMY inputs

The SAMMY inputs containing the experimental configuration for each measured data included in the evaluation work are reported in Figs. 27–42. For Liou's transmission data, the experimental configuration consists of the crunch data, the sample thickness, and related isotopic abundances. In addition to these, detector efficiencies are usually reported for RPI's capture measurements together with parameters for the resolution function.

```
Dy / Total / Liou(75) / ENTRY 10525 / Exp. corrections : background
Dy160     159.925204 0.00001 2.0000E+03    1    1 0  0 0  0         0
FGM
TWENTY
EV
DEBUG
GENERATE PLOT FILE AUTOMATICALLY
DO NOT SOLVE BAYES EQUATIONS
ENERGY UNCERTAINTIES ARE AT END OF LINE
EXPONENTIAL FOLDING
REICH-MOORE FORMALISM IS WANTED
QUANTUM NUMBERS ARE IN PARAMETER FILE
USE NO CUTOFF FOR DERIVATIVES OR CROSS SECTIONS
#IMPLICIT DATA COVARIANCE MATRIX IS INCLUDED

   293.6    202.05    0.0012      0.0000   -0.025
     4.e-2   6
  8.0e+1    3.5e+1     2.4e+2   1.6e+1    5.5e+2    8.0e+0   9.0e+2      4.0e+0
  1.2e+3    2.0e+0     1.0e+3   1.0e+0
  7.45613  8.881e-4                     1.e-2
TRANSMISSION

NUCLIDE MASSES AND ABUNDANCES FOLLOW
155.924284 .00020000 1.0000E-5 0 1
157.924415 .00020000 1.0000E-5 0 2
159.925204 .69460000 1.0000E-5 0 3
160.926939 .17830000 1.0000E-5 0 4 5
161.926805 .06450000 1.0000E-5 0 6 7 8
162.928737 .03550000 1.0000E-5 0 910
163.929181 .02670000 1.0000E-5 0111213

#MISCEllaneous parameters follow
#TZERO 1 1  .00084733 .00100000 1.0001034 .00100000 202.05000
```

Figure 27. SAMMY input for n+^{160}Dy Liou's transmission data.

```
Dy / Total / Liou(75) / ENTRY 10525 / Exp. corrections : background
Dy161     160.926939  0.00001 1.0000E+03    1    1 0  0 0  0         0
FGM
TWENTY
EV
DEBUG
GENERATE PLOT FILE AUTOMATICALLY
DO NOT SOLVE BAYES EQUATIONS
ENERGY UNCERTAINTIES ARE AT END OF LINE
EXPONENTIAL FOLDING
REICH-MOORE FORMALISM IS WANTED
QUANTUM NUMBERS ARE IN PARAMETER FILE
USE NO CUTOFF FOR DERIVATIVES OR CROSS SECTIONS
#IMPLICIT DATA COVARIANCE MATRIX IS INCLUDED

   293.6    202.05    0.0012      0.0000   -0.025
     4.e-2   5
  8.0e+1    3.5e+1     2.4e+2   1.6e+1    5.5e+2    8.0e+0   9.0e+2      4.0e+0
  1.2e+3    1.0e+0
   7.46999  7.451e-3                     1.e-2
TRANSMISSION

NUCLIDE MASSES AND ABUNDANCES FOLLOW
155.924284 .00020000 1.0000E-5 0 1
157.924415 .00020000 1.0000E-5 0 2
159.925204 .00350000 1.0000E-5 0 3
160.926939 .95620000 1.0000E-5 0 4 5
161.926805 .02530000 1.0000E-5 0 6 7 8
162.928737 .00900000 1.0000E-5 0 910
163.929181 .00560000 1.0000E-5 0111213
```

Figure 28. SAMMY input for n+^{161}Dy Liou's transmission thick sample data.

```
Dy / Total / Liou(75) / ENTRY 10525 / Exp. corrections : background
Dy161     160.926939  0.00001 2.0000E+02    1    1 0  0 0  0         0
FGM
TWENTY
EV
DEBUG
GENERATE PLOT FILE AUTOMATICALLY
DO NOT SOLVE BAYES EQUATIONS
ENERGY UNCERTAINTIES ARE AT END OF LINE
EXPONENTIAL FOLDING
REICH-MOORE FORMALISM IS WANTED
QUANTUM NUMBERS ARE IN PARAMETER FILE
USE NO CUTOFF FOR DERIVATIVES OR CROSS SECTIONS
#IMPLICIT DATA COVARIANCE MATRIX IS INCLUDED

   293.6    202.05    0.0012      0.0000   -0.025
     4.e-2   2
  8.0e+1    3.5e+1     2.4e+2   1.6e+1
   7.46999  1.644e-3                    1.e-2
TRANSMISSION

NUCLIDE MASSES AND ABUNDANCES FOLLOW
155.924284 .00020000 1.0000E-5 0 1
157.924415 .00020000 1.0000E-5 0 2
159.925204 .00350000 1.0000E-5 0 3
160.926939 .95620000 1.0000E-5 0 4 5
161.926805 .02530000 1.0000E-5 0 6 7 8
162.928737 .00900000 1.0000E-5 0 910
163.929181 .00560000 1.0000E-5 0111213
```

Figure 29. SAMMY input for n+^{161}Dy Liou's transmission thin sample data.

```
Dy / capture / rpi data / Original filename Dy161.dat ( or very similarly Dy161_
RPI_Cap.txt)
Dy161    160.926939  1.00000 2.0000E+03    1    1 0  0 0  0         0 0
FGM
TWENTY
EV
DEBUG
GENERATE PLOT FILE AUTOMATICALLY
DO NOT SOLVE BAYES EQUATIONS
ENERGY UNCERTAINTIES ARE AT END OF LINE
EXPONENTIAL FOLDING
REICH-MOORE FORMALISM IS WANTED
QUANTUM NUMBERS ARE IN PARAMETER FILE
USE NO CUTOFF FOR DERIVATIVES OR CROSS SECTIONS
INFINITE SLAB
DOUBLE
YIELD
DO NOT SHIFT ENERGY
#IMPLICIT DATA COVARIANCE MATRIX IS INCLUDED

     293.6  25.5686   0.005800 0.0600000  -0.01800     5.0       0.001
   0.01280    4
 99.91198   8.000   499.67926   4.000   999.63580   2.000   9999.79785   1.000
  7.469997 6.359E-4                      1.000E-3
CAPTURE
0.0287000     1.0200       0.0    1.0200       0.0

DETECTOR EFFICIENCIES
1.00000001 0.0000000 0 1
1.00000001 0.0000000 0 2
1.00000000 0.0000000 0 3
1.00000000 0.1000000 0 4 5
0.86405800 0.1000000 0 6 7 8
0.93911600 0.1000000 0 910
0.88117600 0.1000000 0111213

NUCLIDE MASSES AND ABUNDANCES FOLLOW
155.924284 .00020000 1.0000E-5 0 1
157.924415 .00020000 1.0000E-5 0 2
159.925204 .00350000 1.0000E-5 0 3
160.926939 .95660000 1.0000E-5 0 4 5
161.926805 .02530000 1.0000E-5 0 6 7 8
162.928737 .00860000 1.0000E-5 0 910
163.929181 .00560000 1.0000E-5 0111213
```

Figure 30. SAMMY input for n+^{161}Dy RPI's capture data.

```
Dy / Total / Liou(75) / ENTRY 10525 / Exp. corrections : background
Dy162     161.926805  0.00001 1.5000E+04    1    1 0  0 0  0         0
FGM
TWENTY
EV
DEBUG
GENERATE PLOT FILE AUTOMATICALLY
DO NOT SOLVE BAYES EQUATIONS
ENERGY UNCERTAINTIES ARE AT END OF LINE
EXPONENTIAL FOLDING
REICH-MOORE FORMALISM IS WANTED
QUANTUM NUMBERS ARE IN PARAMETER FILE
USE NO CUTOFF FOR DERIVATIVES OR CROSS SECTIONS
#IMPLICIT DATA COVARIANCE MATRIX IS INCLUDED

   293.6    202.05    0.0012      0.0000   -0.025
     4.e-2   6
  8.0e+1    3.5e+1     2.4e+2   1.6e+1    5.5e+2    8.0e+0   9.0e+2      4.0e+0
  1.2e+3    2.0e+0     1.5e+4   1.0e+0
   5.90000  6.934e-3                     1.e-2
TRANSMISSION

NUCLIDE MASSES AND ABUNDANCES FOLLOW
155.924284 .00010000 1.0000E-5 0 1
157.924415 .00010000 1.0000E-5 0 2
159.925204 .00800000 1.0000E-5 0 3
160.926939 .01240000 1.0000E-5 0 4 5
161.926805 .96130000 1.0000E-5 0 6 7 8
162.928737 .01790000 1.0000E-5 0 910
163.929181 .00720000 1.0000E-5 0111213
```

Figure 31. SAMMY input for n+^{162}Dy Liou's transmission thick sample data.

```
Dy / Total / Liou(75) / ENTRY 10525 / Exp. corrections : background
Dy162     161.926805  0.00001 1.5000E+04    1    1 0  0 0  0         0
FGM
TWENTY
EV
DEBUG
GENERATE PLOT FILE AUTOMATICALLY
DO NOT SOLVE BAYES EQUATIONS
ENERGY UNCERTAINTIES ARE AT END OF LINE
EXPONENTIAL FOLDING
REICH-MOORE FORMALISM IS WANTED
QUANTUM NUMBERS ARE IN PARAMETER FILE
USE NO CUTOFF FOR DERIVATIVES OR CROSS SECTIONS
#IMPLICIT DATA COVARIANCE MATRIX IS INCLUDED

   293.6    202.05    0.0012      0.0000   -0.025
     4.e-2   6
  8.0e+1    3.5e+1     2.4e+2   1.6e+1    5.5e+2    8.0e+0   9.0e+2      4.0e+0
  1.2e+3    2.0e+0     3.0e+3   1.0e+0
   5.90000  1.533e-3                     1.e-2
TRANSMISSION

NUCLIDE MASSES AND ABUNDANCES FOLLOW
155.924284 .00010000 1.0000E-5 0 1
157.924415 .00010000 1.0000E-5 0 2
159.925204 .00800000 1.0000E-5 0 3
160.926939 .01240000 1.0000E-5 0 4 5
161.926805 .96130000 1.0000E-5 0 6 7 8
162.928737 .01790000 1.0000E-5 0 910
163.929181 .00720000 1.0000E-5 0111213
```

Figure 32. SAMMY input for n+^{162}Dy Liou's transmission thin sample data.

```
Dy / capture / rpi data / Original filename Dy162.dat ( or very similarly Dy162_
RPI_Cap.txt)
Dy162     161.926805  10.0000 1.0000E+03    1    1 0  0 0  0         0
FGM
TWENTY
EV
DEBUG
GENERATE PLOT FILE AUTOMATICALLY
DO NOT SOLVE BAYES EQUATIONS
ENERGY UNCERTAINTIES ARE AT END OF LINE
EXPONENTIAL FOLDING
REICH-MOORE FORMALISM IS WANTED
QUANTUM NUMBERS ARE IN PARAMETER FILE
USE NO CUTOFF FOR DERIVATIVES OR CROSS SECTIONS
INFINITE SLAB
DOUBLE
YIELD
DO NOT SHIFT ENERGY
#IMPLICIT DATA COVARIANCE MATRIX IS INCLUDED

     293.6  25.5686   0.005800 0.0600000  -0.01800     5.0       0.001
   0.01280    4
 0.999795   256.0   9.9884176   128.0   49.982803   16.00   9999.71582   2.000
  5.900000 6.445E-4                        1.000E-3
CAPTURE
0.0295000     0.7545       0.0    0.7545       0.0

DETECTOR EFFICIENCIES
1.00000001 0.0000000 0 1
1.00000001 0.0000000 0 2
1.00000000 0.0000000 0 3
1.15733000 0.1000000 0 4 5
1.00000000 0.1000000 0 6 7 8
1.08687000 0.1000000 0 910
1.01981000 0.1000000 0111213

NUCLIDE MASSES AND ABUNDANCES FOLLOW
155.924284 .00010000 1.0000E-5 0 1
157.924415 .00010000 1.0000E-5 0 2
159.925204 .00080000 1.0000E-5 0 3
160.926939 .01240000 1.0000E-5 0 4 5
161.926805 .96170000 1.0000E-5 0 6 7 8
162.928737 .01780000 1.0000E-5 0 910
163.929181 .00710000 1.0000E-5 0111213
```

Figure 33. SAMMY input for n+^{162}Dy RPI's capture data.

```
Dy / Total / Liou(75) / ENTRY 10525 / Exp. corrections : background
Dy163      162.92873  0.00001 1.0000E+03    1    1 0  0 0  0         0
FGM
TWENTY
EV
DEBUG
GENERATE PLOT FILE AUTOMATICALLY
DO NOT SOLVE BAYES EQUATIONS
ENERGY UNCERTAINTIES ARE AT END OF LINE
EXPONENTIAL FOLDING
REICH-MOORE FORMALISM IS WANTED
QUANTUM NUMBERS ARE IN PARAMETER FILE
USE NO CUTOFF FOR DERIVATIVES OR CROSS SECTIONS
#IMPLICIT DATA COVARIANCE MATRIX IS INCLUDED

   293.6    202.05    0.0012      0.0000   -0.025
     4.e-2   5
  8.0e+1    3.5e+1     2.4e+2   1.6e+1    5.5e+2    8.0e+0   9.0e+2      4.0e+0
  1.2e+3    1.0e+0
   7.49754  1.403e-3                     1.e-2
TRANSMISSION

NUCLIDE MASSES AND ABUNDANCES FOLLOW
155.924284 .00010000 1.0000E-5 0 1
157.924415 .00010000 1.0000E-5 0 2
159.925197 .00030000 1.0000E-5 0 3
160.926933 .00360000 1.0000E-5 0 4 5
161.926798 .01230000 1.0000E-5 0 6 7 8
162.928731 .96840000 1.0000E-5 0 910
163.929174 .01520000 1.0000E-5 0111213
```

Figure 34. SAMMY input for n+^{163}Dy Liou's transmission data.

```
Dy / capture / rpi data / Original filename Dy163_RPI_Cap.txt
Dy163     162.928737  10.0000 1.0000E+03    1    1 0  0 0  0         0
FGM
TWENTY
EV
DEBUG
GENERATE PLOT FILE AUTOMATICALLY
DO NOT SOLVE BAYES EQUATIONS
ENERGY UNCERTAINTIES ARE AT END OF LINE
EXPONENTIAL FOLDING
REICH-MOORE FORMALISM IS WANTED
QUANTUM NUMBERS ARE IN PARAMETER FILE
USE NO CUTOFF FOR DERIVATIVES OR CROSS SECTIONS
INFINITE SLAB
DOUBLE
YIELD
DO NOT SHIFT ENERGY
#IMPLICIT DATA COVARIANCE MATRIX IS INCLUDED

     293.6  25.5686   0.005800 0.0600000  -0.01800     5.0       0.001
   0.01280    4
 99.91198   8.000   499.67926   4.000   999.63580   2.000   9999.79785   1.000
  7.497540 6.503E-4                     1.000E-3
CAPTURE
0.0289000     1.0300       0.0    1.0300       0.0

DETECTOR EFFICIENCIES
1.00000001 0.0000000 0 1
1.00000001 0.0000000 0 2
1.00000000 0.0000000 0 3
1.06483000 0.1000000 0 4 5
0.92007700 0.1000000 0 6 7 8
1.00000000 0.1000000 0 910
0.93830400 0.1000000 0111213

NUCLIDE MASSES AND ABUNDANCES FOLLOW
155.924284 .00010000 1.0000E-5 0 1
157.924415 .00010000 1.0000E-5 0 2
159.925204 .00030000 1.0000E-5 0 3
160.926939 .03600000 1.0000E-5 0 4 5
161.926805 .01230000 1.0000E-5 0 6 7 8
162.928737 .96860000 1.0000E-5 0 910
163.929181 .01520000 1.0000E-5 0111213
```

Figure 35. SAMMY input for n+^{163}Dy RPI's capture data.

```
Dy / Total / Liou(75) / ENTRY 10525 / Exp. corrections : background
Dy164     163.929181  0.00001 4.0000E+03    1    1 0  0 0  0         0
FGM
TWENTY
EV
DEBUG
GENERATE PLOT FILE AUTOMATICALLY
DO NOT SOLVE BAYES EQUATIONS
ENERGY UNCERTAINTIES ARE AT END OF LINE
EXPONENTIAL FOLDING
REICH-MOORE FORMALISM IS WANTED
QUANTUM NUMBERS ARE IN PARAMETER FILE
USE NO CUTOFF FOR DERIVATIVES OR CROSS SECTIONS
#IMPLICIT DATA COVARIANCE MATRIX IS INCLUDED

   293.6    202.05    0.0012      0.0000   -0.025
     4.e-2   6
  8.0e+1    3.5e+1     2.4e+2   1.6e+1    5.5e+2    8.0e+0   9.0e+2      4.0e+0
  1.2e+3    2.0e+0     1.5e+4   1.0e+0
   7.51121  1.054e-2                     1.e-2
TRANSMISSION

NUCLIDE MASSES AND ABUNDANCES FOLLOW
155.924284 .00010000 1.0000E-5 0 1
157.924415 .00020000 1.0000E-5 0 2
159.925204 .00020000 1.0000E-5 0 3
160.926939 .00150000 1.0000E-5 0 4 5
161.926805 .00350000 1.0000E-5 0 6 7 8
162.928737 .01030000 1.0000E-5 0 910
163.929181 .98420000 1.0000E-5 0111213
```

Figure 36. SAMMY input for n+^{164}Dy Liou's transmission thick sample data.

```
Dy / Total / Liou(75) / ENTRY 10525 / Exp. corrections : background
Dy164     163.929181  0.00001 4.0000E+03    1    1 0  0 0  0         0
FGM
TWENTY
EV
DEBUG
GENERATE PLOT FILE AUTOMATICALLY
DO NOT SOLVE BAYES EQUATIONS
ENERGY UNCERTAINTIES ARE AT END OF LINE
EXPONENTIAL FOLDING
REICH-MOORE FORMALISM IS WANTED
QUANTUM NUMBERS ARE IN PARAMETER FILE
USE NO CUTOFF FOR DERIVATIVES OR CROSS SECTIONS
#IMPLICIT DATA COVARIANCE MATRIX IS INCLUDED

   293.6    202.05    0.0012      0.0000   -0.025
     4.e-2   6
  8.0e+1    3.5e+1     2.4e+2   1.6e+1    5.5e+2    8.0e+0   9.0e+2      4.0e+0
  1.2e+3    2.0e+0     4.0e+3   1.0e+0
   7.51121  2.337e-3                    1.e-2
TRANSMISSION

NUCLIDE MASSES AND ABUNDANCES FOLLOW
155.924284 .00010000 1.0000E-5 0 1
157.924415 .00020000 1.0000E-5 0 2
159.925204 .00020000 1.0000E-5 0 3
160.926939 .00150000 1.0000E-5 0 4 5
161.926805 .00350000 1.0000E-5 0 6 7 8
162.928737 .01030000 1.0000E-5 0 910
163.929181 .98420000 1.0000E-5 0111213
```

Figure 37. SAMMY input for n+^{164}Dy Liou's transmission thin sample data.

```
Dy / capture / rpi data / Original filename Dy164.dat (or very similarly Dy164_R
PI_Cap.txt)
Dy164     163.929182  1.00000 2.0000E+03    1    1 0  0 0  0         0
FGM
TWENTY
EV
DEBUG
GENERATE PLOT FILE AUTOMATICALLY
DO NOT SOLVE BAYES EQUATIONS
ENERGY UNCERTAINTIES ARE AT END OF LINE
EXPONENTIAL FOLDING
REICH-MOORE FORMALISM IS WANTED
QUANTUM NUMBERS ARE IN PARAMETER FILE
USE NO CUTOFF FOR DERIVATIVES OR CROSS SECTIONS
INFINITE SLAB
DOUBLE
YIELD
DO NOT SHIFT ENERGY
#IMPLICIT DATA COVARIANCE MATRIX IS INCLUDED

     293.6  25.5686   0.005800 0.0600000  -0.01800     5.0       0.001
   0.01280    4
 99.91198   8.000   499.67926   4.000   999.63580   2.000   9999.79785   1.000
  7.511213 6.196E-4                     1.000E-3
CAPTURE
0.0310000     0.7855       0.0    0.7855       0.0

DETECTOR EFFICIENCIES
1.00000001 0.0000000 0 1
1.00000001 0.0000000 0 2
1.00000000 0.0000000 0 3
1.13485000 0.1000000 0 4 5
0.98057400 0.1000000 0 6 7 8
1.06575000 0.1000000 0 910
1.00000000 0.1000000 0111213

NUCLIDE MASSES AND ABUNDANCES FOLLOW
155.924284 .00010000 1.0000E-5 0 1
157.924415 .00010000 1.0000E-5 0 2
159.925204 .00010000 1.0000E-5 0 3
160.926940 .00140000 1.0000E-5 0 4 5
161.926805 .00350000 1.0000E-5 0 6 7 8
162.928738 .01030000 1.0000E-5 0 910
163.929181 .98450000 1.0000E-5 0111213
```

Figure 38. SAMMY input for n+^{163}Dy RPI's capture data.

```
Dy / capture / rpi data / Original filename DyNat.dat ( or very similar DyNat_20
mil_RPI_Cap)
Dynat     162.499472  1.00000 1.0000E+03    1    1 0  0 0  0         0
FGM
TWENTY
EV
DEBUG
GENERATE PLOT FILE AUTOMATICALLY
DO NOT SOLVE BAYES EQUATIONS
ENERGY UNCERTAINTIES ARE AT END OF LINE
EXPONENTIAL FOLDING
REICH-MOORE FORMALISM IS WANTED
QUANTUM NUMBERS ARE IN PARAMETER FILE
USE NO CUTOFF FOR DERIVATIVES OR CROSS SECTIONS
DOUBLE
INFINITE SLAB
YIELD
DO NOT SHIFT ENERGY
#IMPLICIT DATA COVARIANCE MATRIX IS INCLUDED

     293.6  25.5686   0.005800 0.0600000  -0.01800     5.0       0.001
   0.01280    4
 99.99477   8.000   499.98755   4.000   999.85242   2.000   9999.69434   1.000
  7.088000 1.6304E-3                       0.00100
CAPTURE
0.0604000     1.9070       0.0 1.9070        0.0

DETECTOR EFFICIENCIES
1.00000001 0.0000000 0 1
1.00000001 0.0000000 0 2
1.00000000 0.0000000 0 3
1.00190000 0.1000000 0 4 5
0.86570000 0.1000000 0 6 7 8
0.94090000 0.1000000 0 910
0.88285000 0.1000000 0111213

NUCLIDE MASSES AND ABUNDANCES FOLLOW
155.924284 .00056000 1.0000E-5 0 1
157.924415 .00095000 1.0000E-5 0 2
159.925204 .02329000 1.0000E-5 0 3
160.926939 .18889000 1.0000E-5 0 4 5
161.926805 .25475000 1.0000E-5 0 6 7 8
162.928737 .24896000 1.0000E-5 0 910
163.929181 .28260000 1.0000E-5 0111213
```

Figure 39. SAMMY input for n+^{nat}Dy RPI's epithermal capture data.

```
Dy / capture / rpi data / Original filename Dy_tcnat_10-mil_CSISRS.twenty
Dynat     162.499472  0.00001 2.0000E+01    1    1 0  0 0  0         0
FGM
TWENTY
EV
DEBUG
GENERATE PLOT FILE AUTOMATICALLY
DO NOT SOLVE BAYES EQUATIONS
ENERGY UNCERTAINTIES ARE AT END OF LINE
EXPONENTIAL FOLDING
REICH-MOORE FORMALISM IS WANTED
QUANTUM NUMBERS ARE IN PARAMETER FILE
USE NO CUTOFF FOR DERIVATIVES OR CROSS SECTIONS
DOUBLE
YIELD
FINITE SLAB
DO NOT SHIFT ENERGY
#IMPLICIT DATA COVARIANCE MATRIX IS INCLUDED

   293.6    25.444    0.0055      0.0000  -1.0
   0.125      3
  0.1237    64.0      4.0459    4.0      20.0051    1.000
   7.50000  8.050e-4
CAPTURE
0.0254000     2.5400          1.67259

NUCLIDE MASSES AND ABUNDANCES FOLLOW
155.924284 .00060000 1.0000E-5 0 1
157.924415 .00100000 1.0000E-5 0 2
159.925204 .02340000 1.0000E-5 0 3
160.926939 .18910000 1.0000E-5 0 4 5
161.926805 .25510000 1.0000E-5 0 6 7 8
162.928737 .24900000 1.0000E-5 0 910
163.929181 .28180000 1.0000E-5 0111213

MISCELLANEOUS PARAMETERS FOLLOW
DELTE 0 00 6.28-5   1.22-5    0.234     0.016     -.038     0.003

DETECTOR EFFICIENCIES
0.83000000 0.0300000 0 1
0.83000000 0.0200000 0 2
0.81500000 0.0150000 0 3
0.90600000 0.0200000 0 4 5
0.80700000 0.0200000 0 6 7 8
0.89400000 0.0150000 0 910
0.78000000 0.0250000 0111213

#0.0254000     1.9000                  ! As in the EXFOR sheets
#0.0254000     2.5400          1.67259 ! As discussed in May 2021 with D. Barry
#   7.50000  8.050e-4                  ! As in the EXFOR sheets
#   7.50000  7.840e-4                  ! As in the Paper
```

Figure 40. SAMMY input for n+^{nat}Dy RPI's thermal capture data.

```
Dysprosium / transmission / rpi data / Original filename Dy_ttnat_10mil_CSISRS.t
wenty
Dynat     162.499472  4.00001 2.0000E+03    1    1 0  0 0  0         0
FGM
TWENTY
EV
GENERATE PLOT FILE AUTOMATICALLY
PRINT THEORETICAL VALUES
PRINT DEBUG INFORMATION
DO NOT SOLVE BAYES EQUATIONS
REICH-MOORE FORMALISM IS WANTED
QUANTUM NUMBERS ARE IN PARAMETER FILE
DO NOT SHIFT RPI RESOLUTION FUNCTION TO CENTER
ENERGY UNCERTAINTIES ARE AT END OF LINE
USE NO CUTOFF FOR DERIVATIVES OR CROSS SECTIONS
#IMPLICIT DATA COVARIANCE MATRIX IS INCLUDED

   293.6    25.597    0.0055      0.0000
   7.50000  7.840e-4
TRANSMISSION

NUCLIDE MASSES AND ABUNDANCES FOLLOW
155.924284 .00060000 1.0000E-5 0 1
157.924415 .00100000 1.0000E-5 0 2
159.925204 .02340000 1.0000E-5 0 3
160.926939 .18910000 1.0000E-5 0 4 5
161.926805 .25510000 1.0000E-5 0 6 7 8
162.928737 .24900000 1.0000E-5 0 910
163.929181 .28180000 1.0000E-5 0111213

RPI RESOLUTION PARAMETERS FOLLOW
BURST 0     60.      0.1
CHANN 0       44.68    500.000     0.100
CHANN 0      262.17     62.500     0.100
CHANN 0     1998.1      31.250     0.100

MISCELLANEOUS PARAMETERS FOLLOW
DELTE 0 00 -1.27-6  4.49-6    0.187     0.063     -.021     0.003
```

Figure 41. SAMMY input for n+^{nat}Dy RPI's epithermal transmission data.

```
Dysprosium / transmission / rpi data / Original filename Dy_ttnat_20mil_CSISRS.t
wenty
Dynat     162.499472  0.00001 2.0000E+01    1    1 0  0 0  0         0
FGM
TWENTY
EV
GENERATE PLOT FILE AUTOMATICALLY
PRINT THEORETICAL VALUES
PRINT DEBUG INFORMATION
DO NOT SOLVE BAYES EQUATIONS
REICH-MOORE FORMALISM IS WANTED
QUANTUM NUMBERS ARE IN PARAMETER FILE
DO NOT SHIFT RPI RESOLUTION FUNCTION TO CENTER
ENERGY UNCERTAINTIES ARE AT END OF LINE
USE NO CUTOFF FOR DERIVATIVES OR CROSS SECTIONS
#IMPLICIT DATA COVARIANCE MATRIX IS INCLUDED

   293.6    14.973    0.0055      0.0000   0.0
   7.50000  1.610e-3
TRANSMISSION

NUCLIDE MASSES AND ABUNDANCES FOLLOW
155.924284 .00060000 1.0000E-5 0 1
157.924415 .00100000 1.0000E-5 0 2
159.925204 .02340000 1.0000E-5 0 3
160.926939 .18910000 1.0000E-5 0 4 5
161.926805 .25510000 1.0000E-5 0 6 7 8
162.928737 .24900000 1.0000E-5 0 910
163.929181 .28180000 1.0000E-5 0111213

RPI RESOLUTION PARAMETERS FOLLOW
BURST 0   2100.     21.
TAU  00000320.936   0.02426   318.461   0.02922   235.721
TAU  00    82.641   0.00625    82.004   0.00752    60.698
LAMBD00000 679.984  -226.205   21.009
LAMBD      146.197    48.634    4.517
A1   00000 -.000780 0.02407   -.000630  3.531     0.00112
A1          .00005  0.0        .0       0.0       0.00006
EXPON00000 935.91    -69.068   .005     0.39485   0.00075
EXPON        0.801     0.396   .00001   0.00042   0.00002
CHANN 0      0.1096     32000.    0.100
CHANN 0      5.301       2000.    0.100
CHANN 0      19.94        500.    0.100

NORMAlization and "constant" background follow
1.00671608-.00625250-.00045116 0.        0.        0.        0 0 0 0 0 0
.010000000 .00100000 .00100000 0.        0.        0.
```

Figure 42. SAMMY input for n+^{nat}Dy RPI's thermal transmission data.

APPENDIX B. Resonance parameters

The SAMMY parameters file containing the particle-pair definitions, spin group information, and resonance parameters each Dy isotope is shown in Fig. 43. The multiplication factors to calibrate the evaluated uncertainties are reported in Fig. 44. The details on the format of both files can be found in the SAMMY manual [9].

```
PARTICLE PAIR DEFINITIONS
Name=156Dy+n      Particle a=neutron       Particle b=156Dy
     Za= 0        Zb=66          Pent=1     Shift=0
     Sa=  0.5     Sb=   0.0     Ma=     1.00866492     Mb=   155.92428359
Name=158Dy+n      Particle a=neutron       Particle b=158Dy
     Za= 0        Zb=66          Pent=1     Shift=0
     Sa=  0.5     Sb=   0.0     Ma=     1.00866492     Mb=   157.92441482
Name=160Dy+n      Particle a=neutron       Particle b=160Dy
     Za= 0        Zb=66          Pent=1     Shift=0
     Sa=  0.5     Sb=   0.0     Ma=     1.00866492     Mb=   159.92520358
Name=161Dy+n      Particle a=neutron       Particle b=161Dy
     Za= 0        Zb=66          Pent=1     Shift=0
     Sa=  0.5     Sb=   2.5     Ma=     1.00866492     Mb=   160.92693943
Name=162Dy+n      Particle a=neutron       Particle b=162Dy
     Za= 0        Zb=66          Pent=1     Shift=0
     Sa=  0.5     Sb=   0.0     Ma=     1.00866492     Mb=   161.92680451
Name=163Dy+n      Particle a=neutron       Particle b=163Dy
     Za= 0        Zb=66          Pent=1     Shift=0
     Sa=  0.5     Sb=  -2.5     Ma=     1.00866492     Mb=   162.92873722
Name=164Dy+n      Particle a=neutron       Particle b=164Dy
     Za= 0        Zb=66          Pent=1     Shift=0
     Sa=  0.5     Sb=   0.0     Ma=     1.00866492     Mb=   163.92918082

SPIN GROUPS
  1      1    0  0.5 0.0006000
    1  156Dy+n     0  0.5
  2      1    0  0.5 0.0010000
    1  158Dy+n     0  0.5
  3      1    0  0.5 0.0234000
    1  160Dy+n     0  0.5
  4      1    0  2.0 0.1891000
    1  161Dy+n     0  2.0
  5      1    0  3.0 0.1891000
    1  161Dy+n     0  3.0
  6      1    0  0.5 0.2551000
    1  162Dy+n     0  0.5
  7      1    0 -0.5 0.2551000
    1  162Dy+n     1  0.5
  8      1    0 -1.5 0.2551000
    1  162Dy+n     1  0.5
  9      1    0 -2.0 0.2490000
    1  163Dy+n     0 -2.0
 10      1    0 -3.0 0.2490000
    1  163Dy+n     0 -3.0
 11      1    0  0.5 0.2818000
    1  164Dy+n     0  0.5
 12      1    0 -0.5 0.2818000
    1  164Dy+n     1  0.5
 13      1    0 -1.5 0.2818000
    1  164Dy+n     1  0.5

RESONANCES are listed next
2.150000000 83.6000000 .200000000                       1 1 1     1
3.210000000 83.6000000 .800000000                       1 1 1     1
9.190000000 83.6000000 .600000000                       1 1 1     1
15.20000000 83.6000000 4.60000000                       1 1 1     1
17.40000000 83.6000000 .320000000                       1 1 1     1
17.70000000 83.6000000 .100000000                       1 1 1     1
19.60000000 83.6000000 9.00000000                       1 1 1     1
24.50000000 83.6000000 2.40000000                       1 1 1     1
27.40000000 83.6000000 .400000000                       1 1 1     1
28.10000000 83.6000000 .400000000                       1 1 1     1
29.30000000 83.6000000 8.70000000                       1 1 1     1
36.00000000 83.6000000 9.00000000                       1 1 1     1
37.80000000 83.6000000 .400000000                       1 1 1     1
38.60000000 83.6000000 .400000000                       1 1 1     1
46.90000000 83.6000000 14.0000000                       1 1 1     1
52.00000000 83.6000000 16.0000000                       1 1 1     1
68.60000000 83.6000000 54.0000000                       1 1 1     1
85.50000000 83.6000000 15.0000000                       1 1 1     1
90.90000000 83.6000000 42.0000000                       1 1 1     1
-2.00000000 85.0000000 .670000000                       1 1 1     2
38.00000000 90.0000000 22.0000000                       1 1 1     2
45.60000000 90.0000000 39.0000000                       1 1 1     2
86.00000000 90.0000000 81.0000000                       1 1 1     2
-601.812400 103.089300 9545.25600                       1 1 1     3
-51.9874700 99.5353900 326.191200                       1 1 1     3
-14.3017500 88.5602100 9.05126800                       1 1 1     3
1.807561000 102.553100 .186961800                       1 1 1     3
10.44202000 64.6800200 21.1828400                       1 1 1     3
20.41273000 76.6656400 42.7773100                       1 1 1     3
34.92342000 105.737500 1.21132600                       1 1 1     3
73.14351000 105.770600 7.04259300                       1 1 1     3
85.63345000 97.4434000 100.662100                       1 1 1     3
115.5734000 105.802100 2.04259600                       1 1 1     3
136.4542000 95.9104700 26.6468000                       1 1 1     3
155.7083000 103.490600 79.2620800                       1 1 1     3
178.2808000 120.114100 30.0461600                       1 1 1     3
202.2017000 105.631800 31.7822800                       1 1 1     3
246.3273000 105.805300 8.77651500                       1 1 1     3
271.9806000 105.799700 4.35647200                       1 1 1     3
320.8443000 105.804900 13.0409800                       1 1 1     3
341.2202000 105.960400 390.722400                       1 1 1     3
379.4751000 104.064000 293.506400                       1 1 1     3
394.4460000 105.791800 60.0354600                       1 1 1     3
398.7371000 102.958900 206.299000                       1 1 1     3
429.6930000 109.116700 112.786500                       1 1 1     3
522.5569000 105.604200 133.750900                       1 1 1     3
577.2397000 100.097300 36.0894000                       1 1 1     3
591.0122000 105.801000 8.52213000                       1 1 1     3
625.7669000 105.800600 8.03462000                       1 1 1     3
653.5175000 105.799800 5.63304000                       1 1 1     3
679.3814000 107.053900 741.073900                       1 1 1     3
704.0336000 109.233400 912.992500                       1 1 1     3
729.4384000 120.525200 113.703200                       1 1 1     3
737.2087000 108.497600 1276.02300                       1 1 1     3
817.5843000 105.839900 32.1062200                       1 1 1     3
844.8794000 106.222400 110.563900                       1 1 1     3
868.9198000 107.004200 157.302700                       1 1 1     3
889.0758000 105.800300 17.9273500                       1 1 1     3
972.2005000 105.800100 6.91394400                       1 1 1     3
988.7365000 106.249100 88.5005400                       1 1 1     3
1053.601000 105.800300 12.9999100                       1 1 1     3
1086.312000 105.808400 691.172900                       1 1 1     3
1103.366000 105.800500 24.9043600                       1 1 1     3
1133.991000 105.804700 165.026500                       1 1 1     3
1139.208000 105.799800 8.10034700                       1 1 1     3
1161.497000 105.800300 21.9984500                       1 1 1     3
1201.475000 105.799700 31.0044000                       1 1 1     3
1244.516000 105.799900 45.0121100                       1 1 1     3
1279.568000 105.800200 17.0021600                       1 1 1     3
1313.753000 105.813300 280.538000                       1 1 1     3
1367.317000 105.800300 17.9992500                       1 1 1     3
1401.970000 105.803400 135.064600                       1 1 1     3
1412.064000 105.807500 108.981500                       1 1 1     3
1437.673000 105.811600 177.973300                       1 1 1     3
1495.467000 105.806500 200.138900                       1 1 1     3
1542.079000 105.807800 129.955400                       1 1 1     3
1592.631000 105.825100 378.799500                       1 1 1     3
1625.259000 105.800100 13.0000200                       1 1 1     3
1648.761000 105.821000 308.503700                       1 1 1     3
1710.658000 105.815600 309.454700                       1 1 1     3
1721.509000 105.813700 259.643800                       1 1 1     3
1746.396000 105.800500 42.0068200                       1 1 1     3
```

1763.518000	105.800300	25.9997800	1	1	1	3
1785.653000	105.800900	54.9959900	1	1	1	3
1829.586000	105.805800	149.865800	1	1	1	3
1862.719000	105.836500	1295.73800	1	1	1	3
1874.759000	105.805100	159.907000	1	1	1	3
1899.775000	105.809300	279.634500	1	1	1	3
1938.419000	105.822500	618.052400	1	1	1	3
1944.423000	105.808600	239.829700	1	1	1	3
1994.681000	105.805800	249.863000	1	1	1	3
2022.987000	109.956000	662.618600	1	1	1	3
2586.073000	109.151400	22795.4800	1	1	1	3
-369.478000	120.003000	1978.80600	1	1	1	5
-360.669400	120.002400	2454.73200	1	1	1	4
-110.439600	120.001400	44.5552000	1	1	1	5
-19.8295400	119.931900	29.8789000	1	1	1	4
-2.50386400	150.307300	15.3683500	1	1	1	5
2.712675000	109.695900	.631192200	1	1	1	5
3.687048000	113.382700	2.25763200	1	1	1	4
4.323758000	104.497900	1.57775500	1	1	1	4
7.734227000	117.182000	.562243300	1	1	1	5
10.30012000	105.125400	.258270800	1	1	1	4
10.85972000	108.842900	.497382700	1	1	1	5
14.31089000	137.348300	8.33913000	1	1	1	4
16.69933000	121.627200	7.52319000	1	1	1	5
18.49541000	131.146600	10.2977900	1	1	1	4
20.19228000	106.944600	.257904900	1	1	1	4
25.20309000	102.234900	1.53937700	1	1	1	4
29.06393000	125.596500	3.36276300	1	1	1	4
29.93476000	115.745800	.933760300	1	1	1	5
35.74452000	106.539200	2.41911900	1	1	1	5
37.73650000	117.790800	11.6069400	1	1	1	5
38.54457000	109.343000	17.0898300	1	1	1	5
43.30698000	115.653100	13.5006000	1	1	1	5
45.17476000	98.7841300	24.3911000	1	1	1	4
50.89538000	93.1077100	4.07065700	1	1	1	5
51.73043000	120.207200	25.4950700	1	1	1	4
52.24929000	106.819300	1.39240300	1	1	1	5
55.22112000	110.939600	10.0444200	1	1	1	4
59.64267000	106.906600	6.16046400	1	1	1	4
61.43246000	140.845000	9.69856600	1	1	1	4
63.67814000	104.997100	4.41022000	1	1	1	5
67.55024000	106.805000	.118959400	1	1	1	4
71.54195000	112.138700	2.44585600	1	1	1	4
73.20849000	106.761900	5.40130500	1	1	1	4
76.69097000	112.105700	2.04531500	1	1	1	4
77.23483000	106.841900	2.29338200	1	1	1	5
78.13065000	106.815800	.462776100	1	1	1	5
82.32334000	106.870700	3.94085600	1	1	1	4
85.10764000	106.807300	5.47275200	1	1	1	5
88.80316000	106.185200	13.2530500	1	1	1	5
91.11406000	106.858800	1.28461600	1	1	1	4
93.31960000	110.001300	23.8158000	1	1	1	5
95.24622000	106.746400	2.48522800	1	1	1	5
101.3796000	96.3485100	15.1121600	1	1	1	4
102.4405000	106.801800	.700308700	1	1	1	4
104.1791000	106.788400	.627119000	1	1	1	5
105.1008000	106.852200	7.28910300	1	1	1	4
110.5495000	106.916700	9.62052400	1	1	1	5
112.4408000	106.924900	11.6142700	1	1	1	4
113.4061000	106.745200	2.29147200	1	1	1	4
118.4568000	106.853200	8.61823500	1	1	1	4
120.5927000	106.831500	8.67418100	1	1	1	4
124.7077000	119.809800	73.0160200	1	1	1	4
127.6016000	106.816000	2.09899100	1	1	1	5
131.2453000	106.864200	6.55183700	1	1	1	5
137.9754000	112.141400	3.31008400	1	1	1	4
138.4879000	120.073400	13.7238700	1	1	1	5

142.9055000	106.821500	11.5790100	1	1	1	4
144.8194000	106.825200	4.52199400	1	1	1	4
149.4107000	106.803700	3.17701100	1	1	1	5
153.8808000	106.806500	10.8729300	1	1	1	4
155.1150000	112.138400	2.72761200	1	1	1	4
156.8814000	106.826800	7.36876200	1	1	1	4
162.7238000	122.376200	43.7483600	1	1	1	5
165.8622000	112.121400	3.44888800	1	1	1	5
166.6509000	112.547700	40.8546800	1	1	1	4
168.6873000	110.687400	84.8816800	1	1	1	4
170.2053000	106.821400	9.72967100	1	1	1	4
172.8663000	106.871000	13.5240500	1	1	1	5
175.3105000	106.875500	12.7936500	1	1	1	5
176.3391000	106.804000	7.95917100	1	1	1	5
176.9720000	112.128700	7.35181100	1	1	1	4
179.1493000	110.104100	20.6460300	1	1	1	5
183.8006000	108.653000	22.4429900	1	1	1	5
184.5243000	112.112300	7.17414600	1	1	1	4
189.3596000	116.194100	35.0865600	1	1	1	4
191.1019000	106.817500	6.96155000	1	1	1	4
193.0889000	106.789100	1.76674500	1	1	1	4
194.5327000	106.934400	17.5349100	1	1	1	5
197.4077000	102.587100	24.4101800	1	1	1	4
202.9763000	109.338000	27.8469900	1	1	1	4
206.0599000	122.714500	37.9362200	1	1	1	4
208.6430000	106.807800	10.8448300	1	1	1	4
209.4243000	112.142800	3.08560900	1	1	1	4
210.6257000	104.916100	33.2454700	1	1	1	4
212.1008000	106.841200	12.2785700	1	1	1	5
214.2068000	112.275100	28.0686400	1	1	1	5
224.3569000	106.807700	5.19085800	1	1	1	4
227.8804000	108.306100	22.8109500	1	1	1	5
235.5495000	107.036500	23.8407700	1	1	1	4
236.5131000	112.127100	6.09041900	1	1	1	4
239.1643000	106.807000	3.68480200	1	1	1	5
240.9129000	106.797800	5.37602100	1	1	1	4
242.5629000	106.845400	13.1179400	1	1	1	5
245.3449000	109.853100	23.4120000	1	1	1	5
251.7103000	106.788100	3.68978000	1	1	1	4
256.8394000	106.795200	2.15915400	1	1	1	4
258.9109000	106.832200	9.07186200	1	1	1	5
261.2872000	112.306000	26.4390800	1	1	1	4
263.9206000	134.092800	116.706600	1	1	1	4
265.7124000	106.832400	17.2960300	1	1	1	4
267.9505000	106.813600	5.85747400	1	1	1	5
274.4548000	112.203700	17.3217900	1	1	1	4
275.8329000	101.762000	51.0604700	1	1	1	5
283.7079000	106.795400	5.08360600	1	1	1	5
287.5723000	106.801700	3.59076200	1	1	1	5
288.5944000	112.125600	2.49706600	1	1	1	5
292.1282000	106.802600	4.68681400	1	1	1	4
293.9252000	106.829900	10.5399900	1	1	1	5
295.6541000	106.814700	2.95773800	1	1	1	4
300.1008000	112.927900	31.2041200	1	1	1	5
302.4910000	106.819500	3.88901100	1	1	1	5
305.4751000	115.905300	65.8478700	1	1	1	5
311.8873000	111.368300	23.8853500	1	1	1	5
314.7889000	110.116900	38.5044700	1	1	1	4
316.0604000	106.801900	15.8061700	1	1	1	5
319.8596000	137.763300	46.4631300	1	1	1	4
328.7139000	106.801500	2.46596400	1	1	1	5
331.5280000	106.796800	7.62650100	1	1	1	4
338.0714000	172.371000	360.356000	1	1	1	4
343.6492000	105.868100	27.3144100	1	1	1	4
349.6813000	106.801200	5.65640300	1	1	1	5
362.1496000	137.433700	171.426100	1	1	1	4
378.4542000	106.806700	3.27380900	1	1	1	5

381.1557000	106.789100	11.2801600	1	1	1	4
382.9534000	98.9753100	42.8839600	1	1	1	5
384.1581000	112.152300	15.0855200	1	1	1	4
389.4056000	106.804800	4.62485400	1	1	1	5
392.7245000	124.570800	51.5039400	1	1	1	5
396.5137000	96.9572300	27.1215400	1	1	1	5
400.5436000	106.800100	2.03229300	1	1	1	4
403.1319000	106.796800	4.66227000	1	1	1	4
404.0132000	106.801400	2.64421200	1	1	1	5
415.5933000	107.315900	40.5065900	1	1	1	4
420.2279000	106.850800	20.5155100	1	1	1	5
424.9701000	128.404800	111.088200	1	1	1	4
428.4009000	108.613400	39.5970300	1	1	1	5
432.7014000	106.795400	10.2883600	1	1	1	5
435.1947000	106.800900	17.5727700	1	1	1	4
438.9950000	106.800200	5.95016100	1	1	1	4
440.3448000	106.801700	5.91256300	1	1	1	4
442.5135000	106.809100	8.74468100	1	1	1	5
444.0325000	112.126400	5.42944300	1	1	1	5
445.5477000	105.722800	29.3149000	1	1	1	5
447.9812000	106.812900	31.1180500	1	1	1	4
450.6004000	106.856000	26.4443900	1	1	1	5
454.9733000	106.810700	18.2520300	1	1	1	4
459.2719000	117.515500	62.1757900	1	1	1	4
462.7117000	119.262100	100.080000	1	1	1	4
472.6230000	110.884100	50.2083800	1	1	1	4
474.4359000	112.129600	16.3329000	1	1	1	4
475.9301000	104.832600	50.5404100	1	1	1	5
477.7888000	109.823600	85.8760500	1	1	1	5
482.7931000	106.798700	9.05654800	1	1	1	4
490.0371000	106.804600	4.99124600	1	1	1	4
497.7072000	118.167000	29.9562800	1	1	1	5
501.3226000	106.805900	5.99460900	1	1	1	5
504.1206000	106.808200	13.4735500	1	1	1	5
505.4551000	106.813200	15.6642300	1	1	1	5
507.1386000	112.940600	33.9535100	1	1	1	4
511.8916000	112.136500	7.25903800	1	1	1	4
514.4885000	111.568600	52.3866300	1	1	1	4
517.5884000	104.143000	37.2568000	1	1	1	4
519.8613000	113.208700	42.1428200	1	1	1	4
527.3779000	104.020000	29.1827900	1	1	1	4
530.5742000	106.799300	14.9756600	1	1	1	4
535.5250000	118.403100	58.5461700	1	1	1	4
539.7034000	93.5779700	37.7885200	1	1	1	4
540.7983000	112.120700	18.8633500	1	1	1	4
543.5677000	106.804600	7.87593900	1	1	1	4
545.5072000	109.346600	25.3964400	1	1	1	5
553.1371000	106.815000	19.3418900	1	1	1	5
555.2404000	106.802200	5.67987600	1	1	1	5
559.8280000	106.798000	3.56021500	1	1	1	5
562.4469000	107.272800	60.9739300	1	1	1	4
566.4860000	104.410700	26.3139900	1	1	1	5
581.9578000	106.202100	60.7064300	1	1	1	5
584.8814000	106.805800	12.1238700	1	1	1	4
591.4199000	106.800500	2.78745000	1	1	1	5
594.5034000	106.815800	12.6335100	1	1	1	5
596.1214000	106.815200	10.3977100	1	1	1	5
599.9294000	121.453400	218.299400	1	1	1	4
602.5905000	106.806300	9.58860400	1	1	1	4
608.6931000	106.809800	11.3751600	1	1	1	5
614.8983000	102.409200	75.2431300	1	1	1	4
619.5608000	112.123100	13.6708500	1	1	1	4
620.8733000	104.004400	64.7001500	1	1	1	5
625.1995000	106.802700	12.1178500	1	1	1	4
630.2911000	107.528300	21.9661800	1	1	1	5
633.2579000	106.794300	7.51354600	1	1	1	5
633.5766000	112.122900	10.3999600	1	1	1	4

635.7767000	106.793800	14.9636400	1	1	1	4
636.7471000	112.127400	9.12066400	1	1	1	4
642.2091000	110.103200	113.410700	1	1	1	4
645.5482000	112.014200	90.3152300	1	1	1	4
648.8384000	106.800300	20.6675100	1	1	1	5
651.1591000	106.804800	9.02734500	1	1	1	4
657.6776000	106.800100	5.96888400	1	1	1	4
665.9708000	106.802400	3.16692300	1	1	1	5
671.0153000	108.303700	113.331200	1	1	1	5
672.7915000	117.072700	76.6249000	1	1	1	4
675.3309000	106.802100	8.19030900	1	1	1	5
677.9879000	106.802600	6.98252000	1	1	1	5
680.7690000	109.766700	90.8019300	1	1	1	4
682.3002000	112.133200	26.0364100	1	1	1	4
687.3352000	112.126100	10.4291400	1	1	1	4
692.2644000	107.099700	42.9414700	1	1	1	4
697.4611000	110.853200	40.2663400	1	1	1	5
699.5654000	106.808600	18.5023700	1	1	1	5
704.4248000	106.802900	6.99468300	1	1	1	4
710.2022000	106.802000	3.16939200	1	1	1	5
713.0609000	108.118200	30.3483000	1	1	1	4
715.3267000	115.063100	92.4282500	1	1	1	4
717.2678000	112.128300	13.0623300	1	1	1	4
719.0641000	112.134500	11.0949500	1	1	1	5
721.5271000	110.465700	53.5367000	1	1	1	5
724.7751000	106.811800	20.4475500	1	1	1	5
730.0507000	109.331700	54.9611600	1	1	1	4
736.7121000	111.392900	62.3967300	1	1	1	4
739.1045000	110.132000	95.1761700	1	1	1	4
741.2897000	108.008800	34.9438900	1	1	1	4
744.1875000	106.130400	25.1925700	1	1	1	5
747.0084000	108.151900	35.4594800	1	1	1	5
750.4396000	108.323000	41.8599800	1	1	1	4
756.4295000	106.799400	9.97140200	1	1	1	4
759.8473000	106.801900	14.4937600	1	1	1	4
763.9422000	106.804200	11.2513800	1	1	1	5
767.0701000	106.805200	10.9266300	1	1	1	5
771.4399000	110.563800	25.8924800	1	1	1	5
773.7674000	108.026800	51.7899500	1	1	1	4
775.6613000	112.122500	23.2787200	1	1	1	4
777.4054000	108.680800	95.1419000	1	1	1	4
780.7464000	123.329600	215.665700	1	1	1	4
784.6266000	106.513100	39.3004100	1	1	1	5
787.1181000	106.797100	12.9818400	1	1	1	5
790.7962000	106.802400	7.41827500	1	1	1	4
798.4779000	106.800700	8.55547400	1	1	1	5
808.2281000	106.803000	16.6996500	1	1	1	5
810.0167000	112.126600	16.5906900	1	1	1	4
813.0687000	105.474000	46.3146600	1	1	1	5
815.0609000	112.125900	22.9671600	1	1	1	5
818.1934000	106.800000	10.4961300	1	1	1	5
820.7333000	106.805000	11.9389600	1	1	1	4
831.9154000	105.266000	63.0762300	1	1	1	4
833.6702000	106.806200	14.4363000	1	1	1	5
836.3655000	105.827100	78.2846900	1	1	1	5
845.2602000	106.799900	13.3213400	1	1	1	5
851.0779000	105.364100	34.2197800	1	1	1	5
856.4492000	106.805600	21.5310600	1	1	1	5
860.7384000	113.057800	81.7515600	1	1	1	5
864.4424000	106.909100	21.8808500	1	1	1	5
867.7579000	111.088500	33.2571900	1	1	1	4
879.0777000	106.801400	10.9083100	1	1	1	4
882.1160000	107.806400	171.037800	1	1	1	4
885.6871000	107.875900	43.4964600	1	1	1	5
893.3324000	107.142100	22.9752800	1	1	1	4
896.9951000	106.801500	8.70494700	1	1	1	4
900.0586000	106.806400	12.3195300	1	1	1	5

903.5611000	106.941400	56.0503800	1	1	1	5
908.6129000	112.134600	12.6141200	1	1	1	5
910.8103000	107.676100	38.4678800	1	1	1	5
915.1551000	115.579000	176.839600	1	1	1	5
918.5390000	107.771200	109.931600	1	1	1	4
923.0907000	106.804200	15.9683100	1	1	1	5
926.0090000	111.757400	93.7104700	1	1	1	4
934.3659000	106.792900	20.6269400	1	1	1	5
941.7550000	106.794600	14.4102500	1	1	1	4
943.6328000	106.973100	62.6023700	1	1	1	4
946.2750000	112.147800	25.4658200	1	1	1	5
948.7555000	109.176000	92.8094400	1	1	1	4
954.4334000	112.140900	19.9239100	1	1	1	5
956.6405000	107.263700	29.3221500	1	1	1	4
959.0277000	107.424400	59.0251700	1	1	1	5
963.7274000	106.801000	10.3255100	1	1	1	5
965.7417000	106.801000	7.71068500	1	1	1	5
972.8908000	112.595600	96.4080000	1	1	1	4
976.3321000	108.163100	34.1854000	1	1	1	5
978.8434000	105.403700	101.151300	1	1	1	5
981.2340000	106.802000	16.9537100	1	1	1	4
990.4427000	114.067200	166.517000	1	1	1	4
993.3752000	106.800300	11.2935000	1	1	1	5
995.7026000	106.802700	7.25090100	1	1	1	4
1009.916000	120.000000	134.371000	1	1	1	5
1256.134000	120.000000	393.658400	1	1	1	4
1345.090000	120.000200	3747.87600	1	1	1	5
1347.108000	120.000200	4621.42300	1	1	1	4
-1255.35300	117.206800	13241.0600	1	1	1	6
-47.4043900	110.907400	38.5820000	1	1	1	6
5.439644000	127.837000	24.4136900	1	1	1	6
71.10805000	83.3876200	452.743800	1	1	1	6
117.2403000	119.814700	12.0193900	1	1	1	6
208.1229000	110.406700	24.8276400	1	1	1	6
223.5205000	114.436700	42.0640000	1	1	1	6
269.4148000	94.1055500	710.009500	1	1	1	6
357.3939000	102.073500	24.9249800	1	1	1	6
413.2313000	85.9599700	153.663600	1	1	1	6
470.3503000	116.830200	9.02017100	1	1	1	6
529.9783000	70.1813600	316.068100	1	1	1	6
632.9597000	89.6454500	1687.79600	1	1	1	6
686.3481000	96.2127800	485.203900	1	1	1	6
717.0901000	100.356800	613.803900	1	1	1	6
766.7905000	87.2880600	864.060700	1	1	1	6
866.8047000	103.654000	2685.32400	1	1	1	6
951.5922000	71.2093700	185.137200	1	1	1	6
1005.201000	111.992900	50.9701300	1	1	1	6
1066.679000	116.803800	31.0339100	1	1	1	6
1110.827000	108.033100	260.193200	1	1	1	6
1261.732000	116.827200	853.732600	1	1	1	6
1360.889000	109.946300	130.034900	1	1	1	6
1431.595000	116.890900	1515.37100	1	1	1	6
1526.744000	105.020500	221.355700	1	1	1	6
1567.875000	116.834900	632.038400	1	1	1	6
1681.119000	116.800700	13.0083500	1	1	1	6
1725.196000	115.012100	108.206100	1	1	1	6
1794.828000	116.797700	18.0184800	1	1	1	6
1835.409000	110.003000	219.457600	1	1	1	6
1936.196000	116.823800	924.158300	1	1	1	6
1950.449000	116.806800	71.0188500	1	1	1	6
2003.857000	116.816800	271.147400	1	1	1	6
2081.959000	116.811700	180.448500	1	1	1	6
2181.442000	116.799600	75.1491100	1	1	1	6
2241.475000	116.832600	953.129900	1	1	1	6
2276.351000	116.816300	808.742300	1	1	1	6
2342.393000	116.806600	771.171800	1	1	1	6
2364.067000	116.799300	420.675200	1	1	1	6

2493.338000	116.786700	418.039000	1	1	1	6
2526.959000	116.802800	220.414900	1	1	1	6
2576.261000	116.799500	170.166900	1	1	1	6
2674.233000	116.804500	720.547900	1	1	1	6
2797.803000	116.824700	2692.02600	1	1	1	6
2848.223000	116.800300	799.772200	1	1	1	6
2886.440000	116.802900	1068.49800	1	1	1	6
2943.725000	116.801000	149.989600	1	1	1	6
2957.217000	116.800800	150.003700	1	1	1	6
3081.081000	116.800800	42.0182500	1	1	1	6
3183.536000	116.800600	120.015900	1	1	1	6
3243.860000	116.803500	738.988100	1	1	1	6
3326.705000	116.803300	260.168500	1	1	1	6
3363.870000	116.801500	229.975300	1	1	1	6
3555.594000	116.795000	2381.53800	1	1	1	6
3624.040000	116.800000	35.0069000	1	1	1	6
3665.811000	116.803800	509.611400	1	1	1	6
3800.222000	116.798100	2883.80600	1	1	1	6
3894.582000	116.800200	39.0040500	1	1	1	6
4012.822000	116.800400	1392.97100	1	1	1	6
4081.819000	116.800300	1394.55500	1	1	1	6
4096.105000	116.800100	389.589100	1	1	1	6
4114.928000	116.800500	2582.39100	1	1	1	6
4239.005000	116.800100	848.410300	1	1	1	6
4273.303000	116.800100	519.426600	1	1	1	6
4393.501000	116.800000	209.916400	1	1	1	6
4452.306000	116.800200	2092.04400	1	1	1	6
4554.900000	116.800000	67.9922600	1	1	1	6
4657.000000	116.800000	95.9856000	1	1	1	6
4785.601000	116.800000	479.667600	1	1	1	6
4844.600000	116.800000	129.976400	1	1	1	6
5032.504000	119.996100	1779.21900	1	1	1	6
6255.305000	119.892300	78659.3900	1	1	1	6
1387.500000	116.800000	2.40000000	1	1	1	8
1483.300000	116.800000	3.50000000	1	1	1	8
2047.600000	116.800000	4.50000000	1	1	1	8
3028.900000	116.800000	9.00000000	1	1	1	8
3270.900000	116.800000	18.0000000	1	1	1	7
3513.800000	116.800000	13.0000000	1	1	1	8
3966.900000	116.800000	13.0000000	1	1	1	8
-584.186700	120.070500	1513.45500	1	1	1	10
-552.738000	120.171300	4151.67100	1	1	1	9
-4.64829800	120.567100	3.19244900	1	1	1	10
1.718878617	101.580971	2.10009344	1	1	1	9
5.896487000	108.516800	.032793660	1	1	1	9
6.257694000	120.879400	.040264060	1	1	1	9
16.24160000	62.2511200	29.0239100	1	1	1	10
19.68895000	114.427100	1.02464100	1	1	1	10
35.80051000	107.274400	13.5988700	1	1	1	9
50.26994000	108.335200	3.35220300	1	1	1	10
55.93295000	136.524100	26.8833800	1	1	1	10
59.05329000	104.516800	106.813100	1	1	1	9
66.14400000	108.445700	8.54483500	1	1	1	10
72.04154000	108.547700	4.36337300	1	1	1	9
75.42876000	108.568800	3.65031100	1	1	1	9
79.02582000	108.431700	20.8604200	1	1	1	9
86.31061000	108.563100	1.25690900	1	1	1	10
94.14237000	108.222200	19.3890700	1	1	1	10
105.8724000	118.880800	66.8361300	1	1	1	10
107.2066000	110.030900	39.4068200	1	1	1	9
120.3983000	108.529900	9.74491800	1	1	1	10
126.6425000	108.688600	16.8567400	1	1	1	10
127.5046000	108.623500	13.2406900	1	1	1	10
135.3777000	108.585400	5.72828900	1	1	1	10
143.4806000	108.545200	16.7510000	1	1	1	9
145.0107000	103.754600	54.2522200	1	1	1	9
155.1077000	99.9663100	106.001300	1	1	1	9

163.8931000	108.528800	11.2000800	1	1	1	10
177.2511000	108.583200	3.73201200	1	1	1	10
185.2036000	108.572900	4.35937200	1	1	1	10
189.0368000	108.596400	4.22452900	1	1	1	9
202.9841000	105.962500	22.1691000	1	1	1	9
205.3569000	100.329900	54.1867200	1	1	1	10
213.8396000	108.601300	6.35007600	1	1	1	10
223.9485000	101.166300	190.920400	1	1	1	9
224.6202000	108.186600	30.0448800	1	1	1	10
233.6697000	108.600900	6.17839400	1	1	1	10
250.7320000	108.606800	15.6419000	1	1	1	10
261.3155000	99.9760100	107.625800	1	1	1	10
268.1567000	98.8800700	133.537000	1	1	1	10
274.3579000	115.936100	37.4991900	1	1	1	9
281.1887000	110.552300	27.8244200	1	1	1	10
289.0532000	94.7451200	145.695200	1	1	1	9
295.9477000	108.595700	7.85981800	1	1	1	9
297.3158000	108.267900	12.9405400	1	1	1	9
298.0892000	92.5848900	92.5263000	1	1	1	9
323.0735000	103.616600	255.973200	1	1	1	10
324.7490000	100.999300	260.120200	1	1	1	10
327.1781000	108.711000	33.9232300	1	1	1	9
329.6652000	108.612000	19.2883500	1	1	1	9
343.0807000	108.634700	20.0278300	1	1	1	10
348.3942000	95.9927100	298.350900	1	1	1	9
368.8199000	134.582400	215.193600	1	1	1	9
375.4251000	108.596400	3.25806400	1	1	1	10
382.4495000	108.593000	6.09037200	1	1	1	9
387.2756000	112.142900	32.9710600	1	1	1	9
390.6223000	89.9603700	45.0655000	1	1	1	10
400.3766000	109.384600	34.5865600	1	1	1	9
403.0535000	108.596500	4.04289500	1	1	1	9
411.3714000	175.671000	629.927600	1	1	1	9
420.8477000	108.599400	2.50380900	1	1	1	10
429.6339000	67.3738000	36.1346700	1	1	1	10
455.1084000	147.802200	75.8308700	1	1	1	10
459.5126000	107.763600	22.4578900	1	1	1	10
465.5376000	108.608300	20.6912800	1	1	1	10
479.4098000	148.501900	85.0241300	1	1	1	9
483.9863000	120.143200	94.8056600	1	1	1	9
502.7254000	108.272000	9.32059200	1	1	1	9
504.4667000	108.263800	22.5339200	1	1	1	9
505.2247000	62.0862800	127.122300	1	1	1	9
516.5177000	114.002800	25.8456500	1	1	1	10
519.3703000	101.205100	19.5291000	1	1	1	9
520.4253000	108.262300	14.1011200	1	1	1	9
533.6283000	122.047300	248.793200	1	1	1	9
542.6806000	125.148800	342.624300	1	1	1	9
564.6313000	87.3671500	76.6732200	1	1	1	9
569.4025000	157.131700	157.703300	1	1	1	9
581.1365000	126.214300	73.2086300	1	1	1	10
594.8218000	112.358600	86.8534700	1	1	1	10
601.5340000	143.858200	199.544400	1	1	1	9
616.2194000	73.0698600	57.2289700	1	1	1	10
621.0201000	122.431600	134.527100	1	1	1	9
632.7412000	95.5685800	155.108000	1	1	1	10
637.5524000	135.694000	196.681700	1	1	1	9
642.4141000	77.2176900	111.842200	1	1	1	10
646.7747000	151.128800	102.098300	1	1	1	10
652.6192000	108.600700	7.40359900	1	1	1	9
666.8271000	108.265200	49.4645200	1	1	1	9
685.2264000	108.272300	6.61804100	1	1	1	10
687.5984000	108.597900	22.2579000	1	1	1	10
693.9699000	108.270100	12.5901300	1	1	1	9
696.3310000	118.939000	199.856200	1	1	1	9
710.3155000	108.601700	10.1011900	1	1	1	9
712.8034000	94.2501700	90.3537400	1	1	1	9

714.1198000	108.265900	20.7607000	1	1	1	9
721.7421000	75.1755000	73.0770300	1	1	1	10
732.4391000	108.602900	17.0294400	1	1	1	10
736.4246000	108.599500	17.3933000	1	1	1	10
742.4096000	108.595200	19.7738600	1	1	1	10
747.2669000	108.599300	8.38106200	1	1	1	9
756.4203000	82.3923000	41.7097600	1	1	1	10
758.4774000	108.270700	13.1859900	1	1	1	9
764.5082000	108.600100	22.0335400	1	1	1	9
767.4503000	108.269400	14.9579900	1	1	1	9
770.6395000	108.598600	5.75312700	1	1	1	10
776.7194000	107.978100	24.2917200	1	1	1	10
794.5185000	110.023300	47.4329900	1	1	1	10
796.0833000	108.276100	23.0774300	1	1	1	9
810.2264000	138.754500	362.761200	1	1	1	9
813.1801000	117.840500	69.7845200	1	1	1	9
823.4078000	109.262600	41.9144200	1	1	1	10
831.5636000	109.685200	105.423400	1	1	1	9
834.9037000	108.272200	11.4485000	1	1	1	10
845.9350000	108.597600	11.2424300	1	1	1	10
850.4771000	108.265500	24.1206400	1	1	1	9
851.9654000	108.472900	192.603700	1	1	1	9
858.4091000	112.619100	75.3143100	1	1	1	9
864.0582000	108.265300	26.6709100	1	1	1	10
865.8601000	105.812500	59.3341200	1	1	1	9
874.2411000	108.217600	100.764300	1	1	1	10
900.7551000	97.2678100	210.223200	1	1	1	9
919.1644000	105.014100	73.9916300	1	1	1	10
920.7148000	108.269400	41.1907200	1	1	1	10
930.4786000	98.3948900	240.323000	1	1	1	9
936.0401000	108.791000	32.5148300	1	1	1	10
940.1376000	86.3417000	208.223800	1	1	1	10
949.9583000	103.472200	169.591600	1	1	1	9
954.6061000	108.272400	15.3286100	1	1	1	9
958.1560000	109.495500	31.2926600	1	1	1	10
967.4671000	111.397700	60.7538500	1	1	1	9
973.6790000	120.808200	295.082300	1	1	1	9
980.8597000	108.599500	11.3241100	1	1	1	10
997.3066000	109.807300	66.3128500	1	1	1	9
1007.240000	120.005700	294.928800	1	1	1	9
1275.274000	120.071300	4883.48600	1	1	1	10
1275.499000	120.001100	74.8314500	1	1	1	10
1296.580000	120.087400	8631.93200	1	1	1	9
-2037.04900	83.6000100	46629.7400	1	1	1	11
-102.492300	83.6000500	310.255600	1	1	1	11
-1.87976800	63.5308900	50.0655200	1	1	1	11
147.1067000	90.4412600	832.878300	1	1	1	11
450.5417000	72.6956300	268.867800	1	1	1	11
536.6550000	63.5467500	106.479500	1	1	1	11
549.1917000	114.237000	6.90768600	1	1	1	11
854.3820000	82.3533600	520.078900	1	1	1	11
983.7238000	110.415000	105.845300	1	1	1	11
1052.182000	105.091300	230.530700	1	1	1	11
1207.945000	114.332300	666.624500	1	1	1	11
1324.066000	114.446800	924.968900	1	1	1	11
1588.481000	115.056100	220.317200	1	1	1	11
1644.745000	114.204200	23.0333900	1	1	1	11
1897.085000	114.328600	2037.20200	1	1	1	11
1960.861000	114.303300	1249.56600	1	1	1	11
2065.076000	114.208200	46.1358700	1	1	1	11
2320.222000	114.276300	1905.32200	1	1	1	11
2397.211000	114.236800	421.286600	1	1	1	11
2537.213000	114.242000	659.521700	1	1	1	11
2871.766000	114.278200	2496.20800	1	1	1	11
2970.108000	114.248000	3154.50500	1	1	1	11
3281.885000	114.204100	219.924000	1	1	1	11
3481.973000	114.209600	1876.38600	1	1	1	11

```
3734.771000 114.206200 727.898200                       1 1 1    11
4135.211000 114.200200 488.227100                       1 1 1    11
4231.531000 114.200600 2168.07800                       1 1 1    11
4445.840000 114.200900 4862.07600                       1 1 1    11
4757.601000 114.200000 139.909700                       1 1 1    11
4780.107000 114.200200 1489.77900                       1 1 1    11
4810.150000 114.201400 10285.3900                       1 1 1    11
4954.901000 114.200000 169.879600                       1 1 1    11
5169.907000 114.200200 2083.38400                       1 1 1    11
5211.940000 114.201200 12382.8100                       1 1 1    11
5592.104000 114.200100 1591.85600                       1 1 1    11
5702.501000 114.200000 239.823800                       1 1 1    11
5923.319000 114.200600 10190.7300                       1 1 1    11
6096.803000 114.200100 1791.34900                       1 1 1    11
6109.803000 114.200100 2088.27800                       1 1 1    11
6280.710000 114.200300 6780.55200                       1 1 1    11
6444.703000 114.200100 2287.32300                       1 1 1    11
6621.105000 114.200200 3767.16400                       1 1 1    11
6854.201000 114.200000 1196.92600                       1 1 1    11
6996.301000 114.200000 997.944500                       1 1 1    11
7102.111000 100.000000 1132.60200                       1 1 1    11
9015.633000 100.000000 98653.6500                       1 1 1    11
804.2400000 114.200000 8.80000000                       1 1 1    12
940.9800000 114.200000 2.45000000                       1 1 1    13
1286.500000 114.200000 4.30000000                       1 1 1    12
1405.800000 114.200000 3.20000000                       1 1 1    13
1567.400000 114.200000 4.95000000                       1 1 1    13
1709.000000 114.200000 9.90000000                       1 1 1    12
2038.700000 114.200000 14.5000000                       1 1 1    13
2250.700000 114.200000 4.00000000                       1 1 1    13
2285.100000 114.200000 31.0000000                       1 1 1    12
2352.600000 114.200000 8.00000000                       1 1 1    12
2723.200000 114.200000 27.0000000                       1 1 1    12
2804.400000 114.200000 8.00000000                       1 1 1    13
3048.200000 114.200000 8.50000000                       1 1 1    13
3100.000000 114.200000 9.50000000                       1 1 1    13
3209.000000 114.200000 26.5000000                       1 1 1    13
3416.800000 114.200000 23.5000000                       1 1 1    13
3460.500000 114.200000 28.0000000                       1 1 1    13
3520.300000 114.200000 71.0000000                       1 1 1    12
3621.000000 114.200000 17.0000000                       1 1 1    12
3911.600000 114.200000 17.0000000                       1 1 1    13
4095.800000 114.200000 30.0000000                       1 1 1    13
4348.800000 114.200000 25.5000000                       1 1 1    13
4389.200000 114.200000 14.5000000                       1 1 1    13
4916.000000 114.200000 42.0000000                       1 1 1    13

1.000000000
Channel radii in key-word format
Radii=  7.500000,  7.500000    Flags=0,-1
   Uncertainties=  0.037500,  7.500000
   Group=  1   Chan=  1,
Radii=  7.400000,  7.400000    Flags=0,-1
   Uncertainties=  0.037000,  7.400000
   Group=  2   Chan=  1,
Radii=  7.4561270  7.4561270   Flags=0,-1
   Uncertainties=  0.040000,  7.4561270
   Group=  3   Chan=  1,
Radii=  7.469997,  7.469997    Flags=0,-1
   Uncertainties=  0.040000,  7.469997
   Group=  4   Chan=  1,
   Group=  5   Chan=  1,
Radii=  5.900000,  5.900000    Flags=0,-1
   Uncertainties=  0.030000,  5.900000
   Group=  6   Chan=  1,
   Group=  7   Chan=  1,
   Group=  8   Chan=  1,
```

```
Radii=  7.497540,  7.497540    Flags=0,-1
   Uncertainties=  0.040000,  7.497540
   Group=  9   Chan=  1,
   Group= 10   Chan=  1,
Radii=  7.511213,  7.511213    Flags=0,-1
   Uncertainties=  0.036553,  7.511213
   Group= 11   Chan=  1,
   Group= 12   Chan=  1,
   Group= 13   Chan=  1,

Prior uncertainties in key-word format
   Relative uncertainty = 0.10  Group=1  Ch=1
   Relative uncertainty = 0.10  Group=2  Ch=1
   Relative uncertainty = 0.10  Group=3  Ch=1
   Relative uncertainty = 0.10  Group=4  Ch=1
   Relative uncertainty = 0.10  Group=5  Ch=1
   Relative uncertainty = 0.10  Group=6  Ch=1
   Relative uncertainty = 0.10  Group=7  Ch=1
   Relative uncertainty = 0.10  Group=8  Ch=1
   Relative uncertainty = 0.10  Group=9  Ch=1
   Relative uncertainty = 0.10  Group=10 Ch=1
   Relative uncertainty = 0.10  Group=11 Ch=1
   Relative uncertainty = 0.10  Group=12 Ch=1
   Relative uncertainty = 0.10  Group=13 Ch=1
   Relative uncertainty = 0.10  pp=capture
   Relative uncertainty = 0.005 pp=energy
```

Figure 43. SAMMY parameter file containing particle-pair definition for seven Dy isotopes and related quantum number information. Resonance parameters (energy and resonance widths) are also shown.

```
Multiplication factor to increase uncertainty from 1.e-5 up 0.5 eV
factors defined below for each isotope.
spin group = 1
0.0       1.
0.5       1.

spin group = 2
0.0       1.
0.5       1.

spin group = 3
0.0       1.
0.5       1.

spin group = 4
0.0       3.
10.       3.

spin group = 5
0.0       3.
10.       3.

spin group = 6
0.0       5.
10.       5.

spin group = 7
0.0       1.
0.5       1.

spin group = 8
0.0       1.
0.5       1.

spin group = 9
-3000.0   2.
0.0       2.

spin group = 10
-3000.0   2.
0.0       2.

spin group = 11
-3000.0   10.
0.        10.

spin group = 12
0.0       1.
0.5       1.

spin group = 13
0.0       1.
0.5       1.
```

Figure 44. SAMMY energy dependent uncertainty file containing the multiplication factors applied on a specific energy range defined by the energy levels of a specific isotope.